Available online at www.sciencedirect.com
ScienceDirect
Coordination Chemistry Reviews 251 (2007) 2562–2591
COORDINATION CHEMISTRY REVIEWS
www.elsevier.com/locate/ccr

Review

Coordination chemistry and supramolecular chemistry in mesoporous nanospace

Katsuhiko Ariga [a,*], Ajayan Vinu [b], Jonathan P. Hill [a], Toshiyuki Mori [b]

[a] *Supermolecules Group, National Institute for Materials Science (NIMS), 1-1 Namiki, Tsukuba 305-0044, Japan*
[b] *Nano Ionics Materials Group, Fuel Cell Materials Center, National Institute for Materials Science (NIMS), Japan*

Received 25 December 2006; accepted 28 February 2007
Available online 4 March 2007

Contents

Abstract

Unexplored science and functions can be found within the well-structured confined spaces of mesoporous materials. The structural dimensions of mesoporous materials permit access by functional supermolecules, including coordination complexes, and control of their functionality can be achieved by variation of pore geometry. This review is a comprehensive summary of recent research in coordination chemistry, supramolecular chemistry, and related functions, in relation to mesoporous materials. Examples of molecular bonding, recognition, selection, sensing, catalytic activities, controlled release, biological and bio-medical applications, and photo-electronic functions are included. Flexibility in the design of mesoporous nanospaces is suitable for fundamental research, affording well-defined dimensions and mutual geometries of functional materials. In addition, ease of synthesis stimulates speculation on various kinds of practical applications using mesoporous materials.

Keywords: Mesoporous materials; Supramolecular chemistry; Coordination complex; Molecular sensing; Controlled release; Photo-electronic function

1. Introduction: fundamentals for design of mesoporous nanospace

According to IUPAC classification, mesopore materials are defined as materials of pore diameter in the range 2.0–50.0 nm. Recently, considerable developments in the preparation of well ordered mesoporous materials have triggered research efforts in catalysis, catalyst supports, and adsorbents because of their high-specific surface areas, large specific pore volumes, and narrow distributions of pore diameter [1–7]. However, advantages of these structures are not limited to such application. Mesoporous materials have been recently paid much attention in fundamental research because unexplored science and function can be located in well-structured confined spaces [8–12]. The structural dimensions of mesoporous materials allow not only easy accessibility for functional supermolecules including

* Corresponding author. Tel.: +81 29 860 4597; fax: +81 29 852 4832.
E-mail address: ARIGA.Katsuhiko@nims.go.jp (K. Ariga).

0010-8545/$ – see front matter © 2007 Elsevier B.V. All rights reserved.
doi:10.1016/j.ccr.2007.02.024

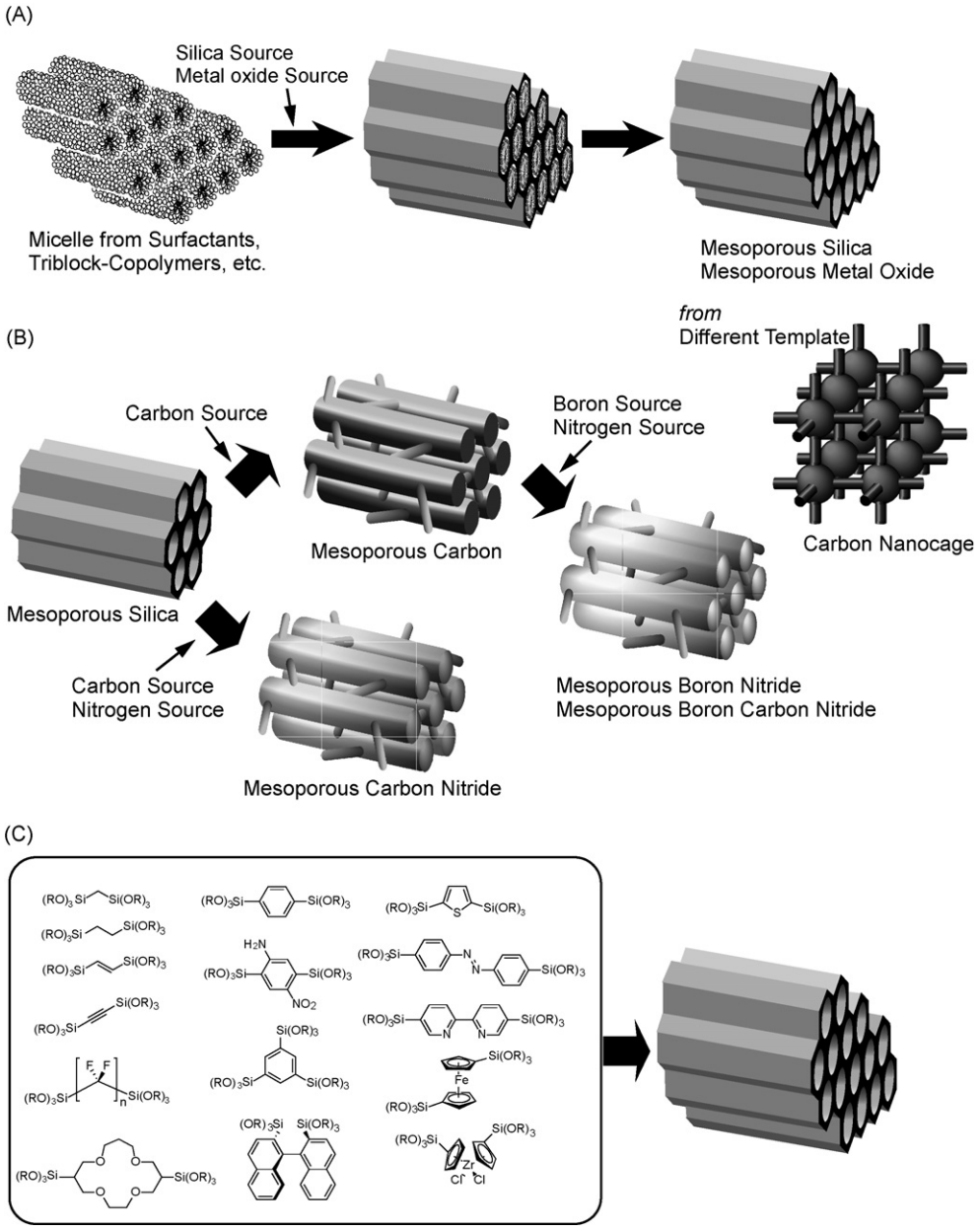

Fig. 1. Outline of syntheses of mesoporous materials: (A) soft-template method; (B) hard-template method and elemental substitution; (C) periodic mesoporous organosilane.

coordination complexes but also controllability of their function by variation of pore geometry. In this review, recent research related to coordination chemistry and supramolecular chemistry in mesoporous nanospaces will be introduced with classification according to functionality.

Prior to a description of coordination chemistry and supramolecular chemistry, fundamental design and preparation methods of mesoporous materials will be briefly summarized. Among the relevant materials, mesoporous silica has been most frequently employed [13–20]. General synthetic methodologies are summarized in Fig. 1. Mesoporous silica materials are prepared essentially using micelle assemblies of surfactants and block-copolymers as soft templates (Fig. 1A). In 1990, Kuroda and coworkers first reported the preparation of mesoporous silica with uniform pore size distribution through intercalation of cetyltrimethylammonium cations into the layered polysilicate kanemite followed by calcination to remove the organic moiety. These materials were named FSM-16 (Folded Sheet Materials) [21,22]. Later, Mobil scientists supplied materials having large uniform pore structures, high specific surface area, with specific pore volume and hexagonal geometry (MCM-41, MCM = Mobil Composition of Matter) [23,24], cubic geometry (MCM-48) [25], or lamellar geometry (MCM-50) [26]. Tanev et al. prepared HMS (Hexagonal Mesoporous Silica) using a neutral amine as template [27], and Bagshaw et al. similarly synthesized a disordered mesoporous material designated as MSU-1 (Michigan State University) using polyethylene oxide (PEO) [28]. Stucky and coworkers developed highly

ordered large pore mesoporous silica SBA-15 (Santa Barbara Amorphous) with thicker pore walls and a two dimensional hexagonal structure using a amphiphilic triblock copolymer of poly(ethylene oxide) and poly(propylene oxide) in highly acidic media [29,30]. The same group also prepared MCF (Meso Cellular Form) type materials where triblock copolymers stabilizing oil in water microemulsions were used as templates [31]. Apart from these materials, mesoporous silica materials with various abbreviations have been developed continuously [32–35]. Similar strategies have also been applied for preparation of mesoporous non-siliceous metal oxides, including TiCh [36–45], Ta_2O_5 [39,46–48], Nb_2O_5 [49,50], ZrO_2 [51–53], Al_2O_3 [54–56], and V_2O_5 [57].

One of the best known non-metal-oxide mesoporous materials is mesoporous carbon, which is a carbon material of regular mesoporous structure [58–65]. Mesoporous carbon materials are synthesized through carbonization within mesoporous silica as a hard template and subsequent selective removal of the silica (Fig. 1B). Ryoo et al. first realized synthesis of ordered mesoporous carbon CMK-1 (Carbon Molecular Sieve from KAIST) using MCM-48 silica as template and sucrose as the carbon source [66]. The first well ordered mesoporous carbon (CMK-3) that was a faithful replica of the template was synthesized using SBA-15 as a template [67]. We have recently developed cage-type mesoporous carbon "nanocage" with extremely high surface area and large pore volume using the replica route (Fig. 1B) [68–70]. Similarly, mesoporous materials other than carbon can be synthesized using other sources for those elements. We have actually succeeded in the preparation of mesoporous carbon nitride by the replica route using combined nitrogen and carbon sources (Fig. 1B) [71]. Furthermore, the novel "elemental substitution" technique for preparation of novel mesoporous nitride materials has been proposed [72]. In this method, elements contained in the original mesoporous materials can be substituted by an element or elements from the exterior at very high temperature. Accordingly, we have prepared mesoporous boron nitride and mesoporous boron carbon-nitride from well-ordered mesoporous carbon (Fig. 1B) [72]. One unique approach to the preparation of mesoporous organic–inorganic hybrids is synthesis of periodic mesoporous organosilicates (PMO), which was independently initiated by three groups (Inagaki group [73–75], Ozin group [76], and Stein group [77]) in 1999 using organic molecules bearing multiple alkoxysilane groups, such as bis(triethoxysilyl)ethene and bis(triethoxysilyl)benzene. As summarized in Fig. 1C, various organic components can be introduced as a PMO pore wall.

Modifications of the mesopore framework and interior have been widely studied (Fig. 2) [78], leading to facile accommodation of functional supramolecular materials including coordination complexes. In the co-condensation method (direct synthesis), an organosilane is hydrolytically condensed with

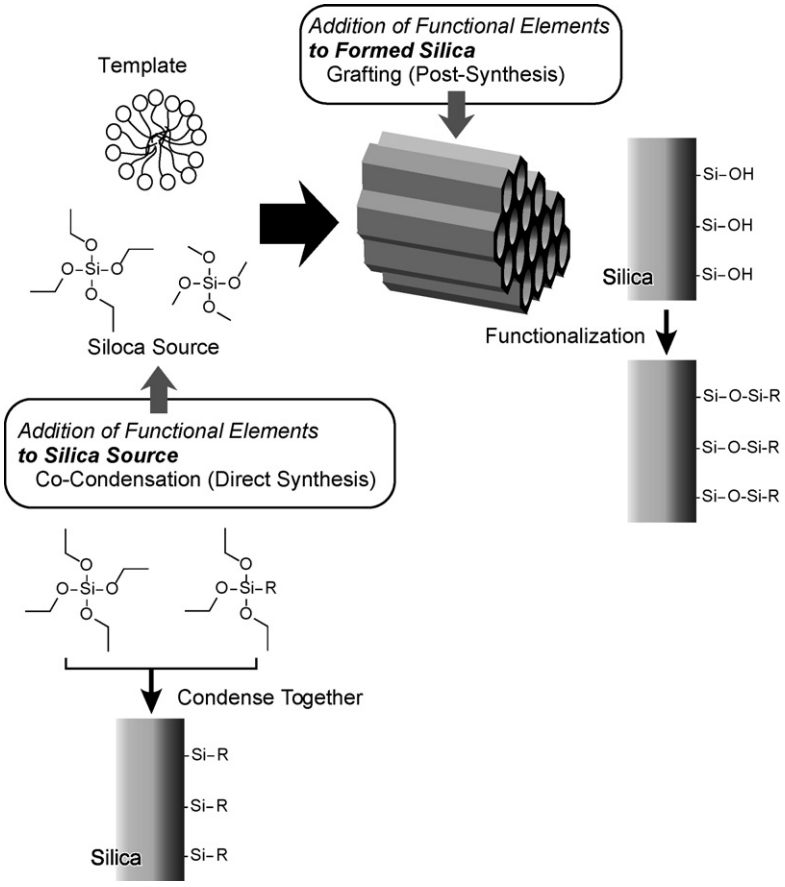

Fig. 2. Outline of modification of mesopore inner space.

conventional silica sources such as tetramethyl orthosilicate and tetraethyl orthosilicate [79–81]. The one-pot pathway of the co-condensation method provides several advantages such as homogeneous distribution of the functional groups and short preparation time. Grafting (post synthesis) is one modification method for pre-synthesized mesoporous silica through direct reaction of organosilanes with the silica surface [82,83]. Distribution of functional groups is sometimes non-uniform but this method is does not compromise the framework structure of the parent mesoporous materials.

2. Functions based on coordination chemistry and supramolecular chemistry

2.1. Binding, recognition, and separation

Mesoporous materials can exhibit excellent adsorption properties with large adsorption capacity because of their high surface areas and specificity relying on complexation chemistry of grafted ligands. Use of functionalized mesoporous materials for molecular binding, recognition, and selection is one of the most promising potential applications.

Functional group-modified mesoporous silica materials are often considered good candidates for use as adsorbents of toxic materials. For example, functionalized mesoporous silicates have been used for adsorption of acidic and basic dye molecules. Most of these dyes are toxic and even carcinogenic, and pose serious threats to human health and the environment. Thus, the textile industry has long been seeking appropriate treatment technologies for efficient removal of dyestuffs. Li and coworkers prepared pyridine-functionalized mesoporous silica via direct condensation of tetraethoxysilane (TEOS) and *N*-(3-(triethoxysilyl)propyl)isonicotinamide (Fig. 3A(a)) and employed the resulting material as an adsorbent for the removal of alizarin red S, reactive brilliant red X-3B and reactive yellow X-RG from waste water [84]. On the basis of the Langmuir analysis, monolayer adsorption capacities were determined to be 143.8, 891.1 and 3369.3 mg of dye per gram of adsorbent for alizarin red S, reactive brilliant red X-3B and reactive yellow X-RG, respectively. The same research group demonstrated the use of mesoporous silica functionalized with a high density of carboxylic groups, suitable as an efficient adsorbent for the removal of basic dyestuffs [85]. It was first synthesized using an organotrialkoxysilane bearing an anhydride moiety that can be easily hydrolyzed to form two carboxylic acid groups (Fig. 3A(b)). Additionally, the important binding activity of a sulfur atom exists within the same functional unit. These mesoporous hybrid materials are suitable as adsorbents for the removal of basic dyestuffs, and exhibit a high adsorption capacity with an extremely rapid adsorption rate. Moreover, these adsorbents can be regenerated by simple washing with acid solution leading to recovery of both the adsorbents and the adsorbed dyes.

The sequestration of environmentally deleterious heavy metal ions has also been the subject of extensive technological research and improved sequestration processes can often result in considerable cost savings. In particular, cadmium, copper, mercury, nickel, and zinc are regarded as some of the most hazardous environmental contaminants. For removal of these metal ions, coordination chemistry within functionalized mesoporous materials can play an important role. Sierra and coworkers synthesized SBA-15 mesoporous silica containing 2-mercaptopyrimidine (Fig. 3A(c)) and demonstrated its capability for adsorption of Cd(II) ion from aqueous media by the batch method [86]. The corresponding binding isotherms provided a maximum adsorption value for Cd(II) of 0.99 mmol g^{-1}.

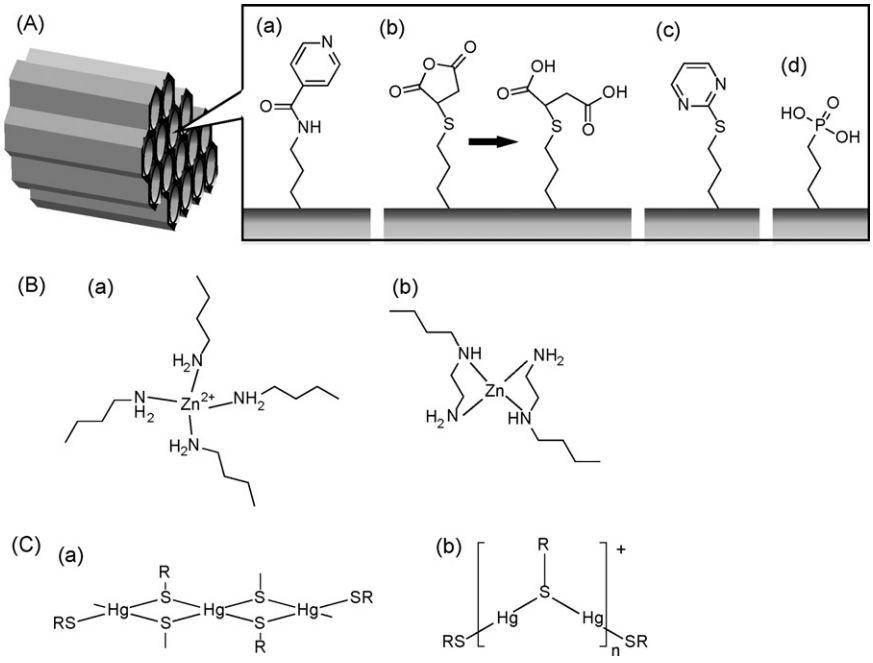

Fig. 3. (A) Binding sites immobilized onto mesoporous silica. (B) Zn(II) ion binding by (a) aminopropyl group and (b) *N*-(2-aminoethyl)-3-aminopropyl group. (C) Binding motifs of thiolate and Hg(II) in mesopores.

On the other hand, the maximum adsorption capacity of the unmodified mesoporous silica was only 0.04 mmol g^{-1}. Only a small amount (0.2 g) of the functionalized mesoporous silica was capable of removing 90% of Cd(II) ions from 5 mL of a 0.03 mM solution at pH 6. Tavlarides and coworkers used mesoporous silica functionalized with phosphonic acid groups for removal of Cr(III) ions (Fig. 3C(d)) [87]. Binding studies using these materials showed an equilibrium Cr(III) adsorption capacity of 82 mg g^{-1} at pH 3.6 and rapid adsorption kinetics. Column adsorption at a high space velocity of 156 h^{-1} is achieved with a minimum effluent chromium concentration of 0.01 mg L^{-1}. Amine-functionalized mesoporous silica can be used as an adsorbent for heavy metal cations through coordination to 3-aminopropyl groups immobilized in the silica mesopores. Wang and coworkers proposed use of mesoporous silica functionalized with *N*-(2-aminoethyl)-3-aminopropyl group as a coordination site for improved removal of heavy metal ions [88]. The amine-functionalized mesoporous silica showed the (Zn/N) molar ratio of ca. 1/4, indicating that Zn(II) ion is coordinated by four amine ligands (Fig. 3B(a)). In contrast, mesoporous silica functionalized with *N*-(2-aminoethyl)-3-aminopropyl group also had (Zn/N) molar ratio of ca. 1/4, where Zn(II) ions within the mesopores is chelated by two aeaptms (Fig. 3B(b)). The metal ions contained in the latter mesoporous silica are so resistant to leaching that its anion-exchange capacity is almost unchanged, even after repeated anion-exchange processes (more than 10 times) because of formation of a stable chelating site. Mercury and its compounds are toxins known to cause neurological impairment in humans and so is of great importance environmentally. Various forms of thiol-functionalized mesostructured silica have been examined as candidates for mercury remediation. In addition, understanding of mercury binding structure has been improved. For example, Billinge et al. applied the atomic pair distribution function analysis obtained from X-ray powder diffraction data, together with Raman spectroscopy, to study a series of thiol-functionalized mesoporous silicates of differing mercaptopropyl content and Hg(II) loading [89]. They proposed the presence of a polymeric HgL_2 (L: ligand) compound in which the mercury ions adopt tetrahedral coordination with bridging thiolates as illustrated in Fig. 3C(a). As the mercury loading is increased to a maximum value of 1.3, the predominant binding mode becomes cationic. The cationic species is also associated with the presence of bridging thiolate ligands, as indicated by the continued presence of a Hg(II)–Hg(II) contact (Fig. 3C(b)). This type of structure accounts for the Hg(II)/S stoichiometry of 1.0. However, the observed Hg(II)/S ratio can be as high as 1.3 suggesting that some of the thiolate ligands bridge three mercury centers. Yeung and coworkers have interpreted the selectivity of metal ions for the functionalized mesoporous silica adsorbent on the basis of a hard-soft, acid–base (HSAB) principle [90]. Pearson's HSAB principle states that hard (Lewis) acids prefer to bind to hard (Lewis) bases and soft (Lewis) acids prefer to bind to soft (Lewis) bases. Fig. 4 summarizes a possible scheme for the adsorption of Ag(I) ions and Cu(II) ions on thiol-functionalized SH-MCM-41 and amine-functionalized NH_2-MCM-41. The grafted mercaptopropyl groups and amino-

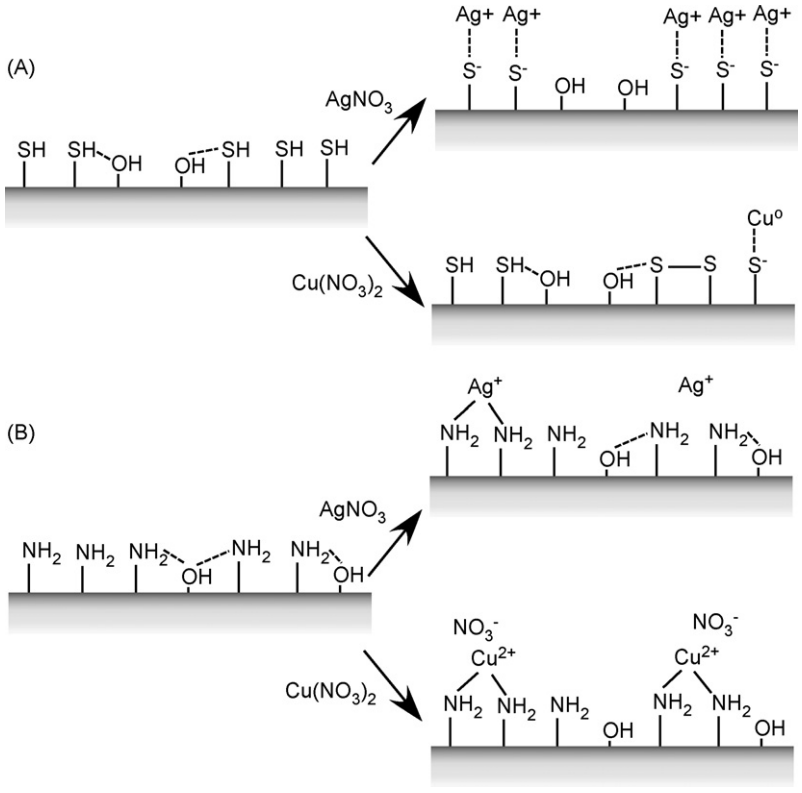

Fig. 4. Selection of metal (Ag(I) and Cu(II)) ions based on hard-soft acid–base principle: (A) thiol-modified surface; (B) amine-modified surface. Reprinted with permission from [90], ©2006, American Chemical Society.

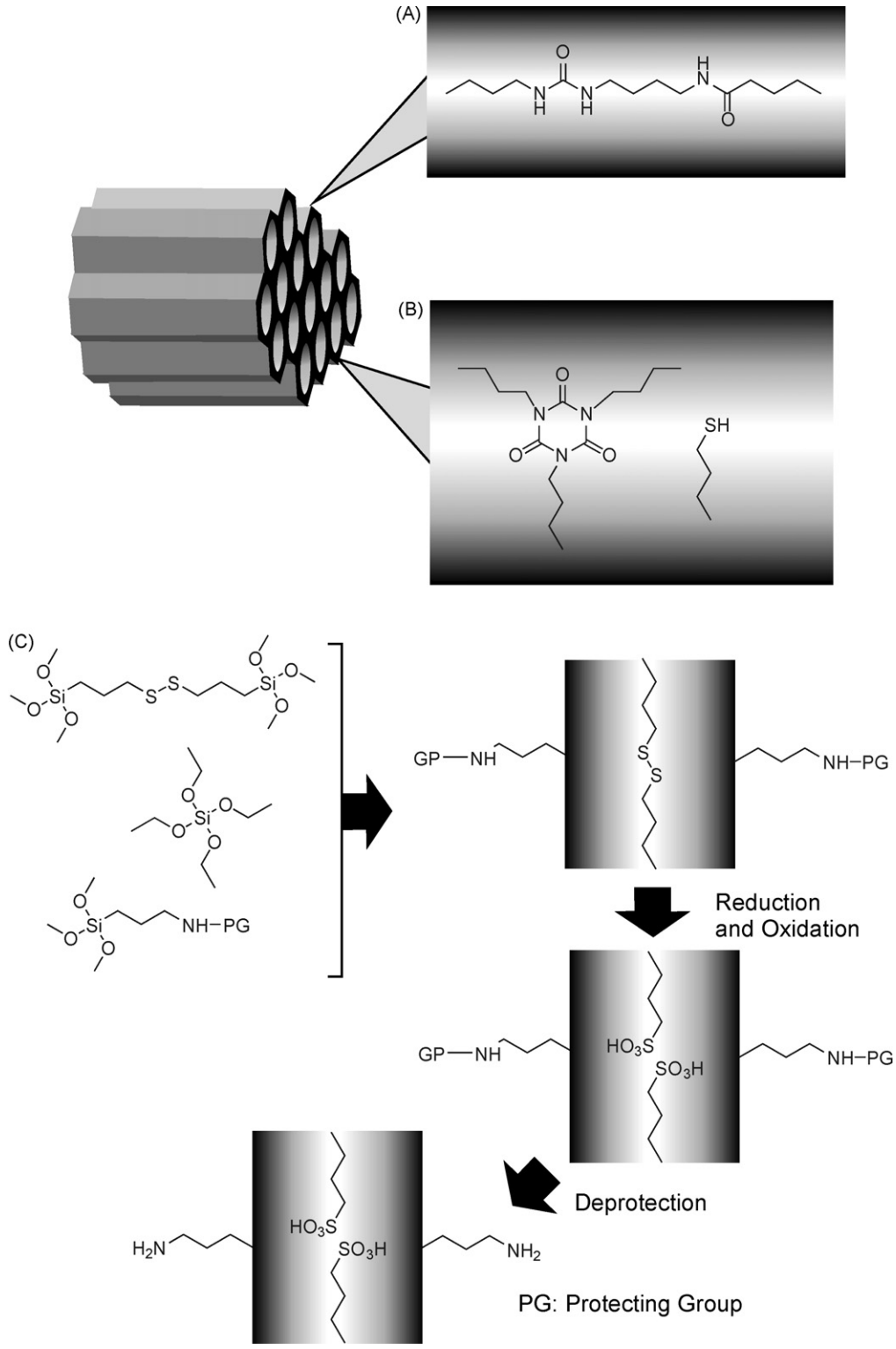

Fig. 5. Introduction of organic binding sites into the framework of mesoporous silica: (A) urea functional group; (B) isocyanurate functional group with thiol group; (C) acid–base bifunctional group.

propyl groups are, respectively, categorized as weak and strong bases. The hard Lewis acid, Cu(II), was removed selectively by NH_2-MCM-41 containing hard Lewis base adsorption sites (i.e., RNH_2), while Ag(I), a soft Lewis acid, was selectively adsorbed by the soft mercaptopropyl base of SH-MCM-41. García and coworkers prepared a urea-containing mesoporous silica and its use for adsorption of Fe(III) ions (Fig. 5A) [91]. The functionalized mesoporous silicates were obtained as PMO type materials using a urea derivative with two alkoxysilane terminals and a conventional silica precursor TEOS. These mesoporous materials have the advantage of containing intraframework urea groups as metal-binding sites thus avoid-

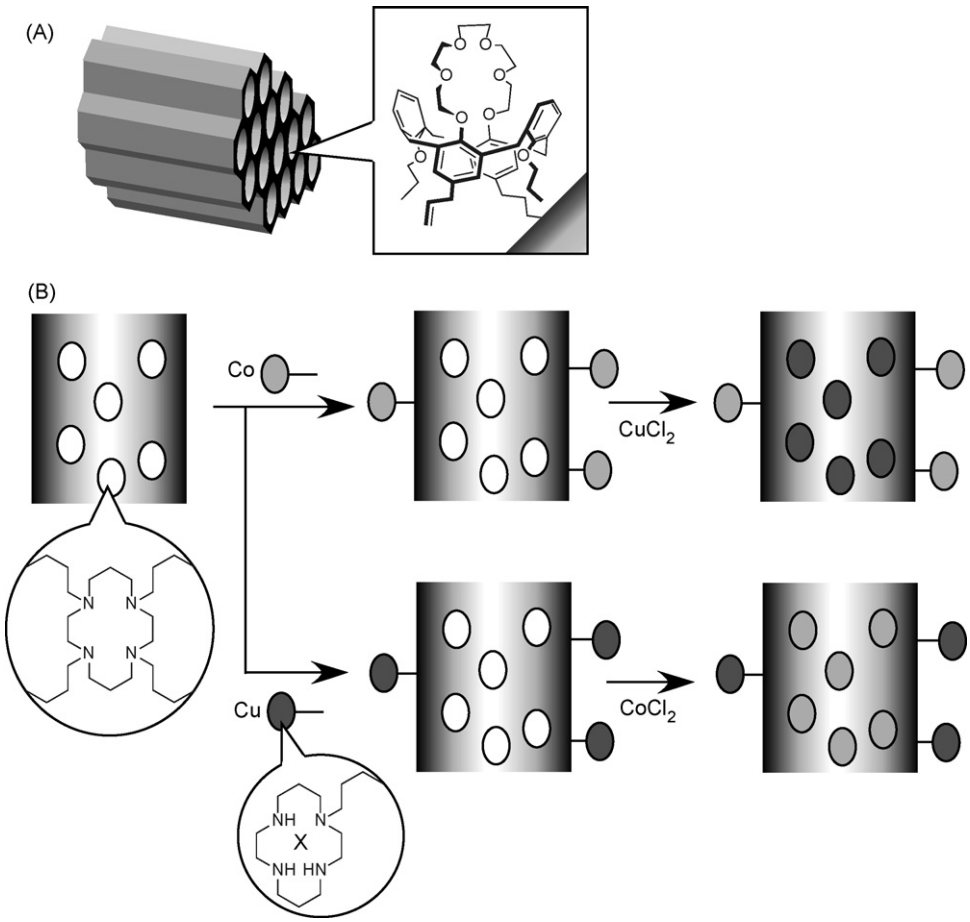

Fig. 6. (A) Calixcrown-immobilized mesoporous silica. (B) Cyclam-immobilized mesoporous silica and site selective binding with Co(II) and Cu(II) ions. Reprinted with permission from [98], ©2003, Royal Society of Chemistry.

ing the problem of channel blocking by the organic moieties. A density of one urea group per ca. 13–16 silicon atoms gave an adsorption capacity of Fe(III) ions for the urea-containing mesoporous silica of 0.19 mmol g^{-1} was determined. Jaroniec and coworkers prepared bifunctional PMOs, with heterocyclic tris[3-(trimethoxysilyl)propyl]isocyanurate rings as bridging groups contained in the siliceous framework and additional mercaptopropyl ligands on the mesopore walls (Fig. 5B), using a direct co-condensation involving 3-mercaptopropyltrimethoxysilane tris[3-(trimethoxysilyl)propyl]isocyanurate [92]. These materials showed metal-chelating properties due to the presence of nitrogen, oxygen and sulfur elements in the incorporated functional groups. For example, high mercury adsorption capacity (4–6 mmol of Hg(II) per gram of the material) was confirmed. This capacity is greater by about 35–90% than the combined adsorption capacities reported for single-component mesoporous silica containing comparable amounts of incorporated ligands. Introduction of multiple kinds of functional groups in mesoporous silica materials can lead to improved metal ion binding. Mehdi and coworkers reported a deft way of separately introducing different functional groups into the framework and at the surface of PMO materials (Fig. 5C) [93,94]. According to the synthetic route depicted in Fig. 5C, the strategy for the preparation of mesoporous organosilica materials leaves acidic groups within the framework and basic groups at the mesopore interior surfaces. Such materials should be ideally suited for acid–base bifunctional catalysis. In addition to the introduced examples, removal of anionic species such as boronate [95] and arsenate [96] were also reported.

Host structures often used in supramolecular chemistry have been immobilized in mesopore nanospaces. For example, Liu et al. reported syntiesis of mesoporous silica containing calixcrown through a co-condensation method (Fig. 6A) [97]. Experiments on the extraction of caesium ions from water in the presence of high concentrations of sodium ions using tie insoluble calixcrown-containing mesoporous organosilicas showed good uptake and high caesium selectivity. These synthetic materials are potentially useful for a wide variety of applications, which require the selective binding of caesium ions, e.g. environmental remediation. Corriu et al., reported synthesis of mesoporous silica materials containing cyclam moieties that can coordinate to metal ions (Fig. 6B) [98,99]. The materials strongly chelate metal ions at two different sites, one in the framework and the other in the pore channels, without displacement of one by the other. This is possible because of the difference in chelating powers between *N*-tetrasubstituted and *N*-monosubstituted cyclam moieties. Thus, it is possible to incorporate two different physical properties such as magnetism and photo luminescence in these materials. As reported by Reyé and coworkers, immobilization of Co-salen and Co-fluomine onto ordered mesoporous

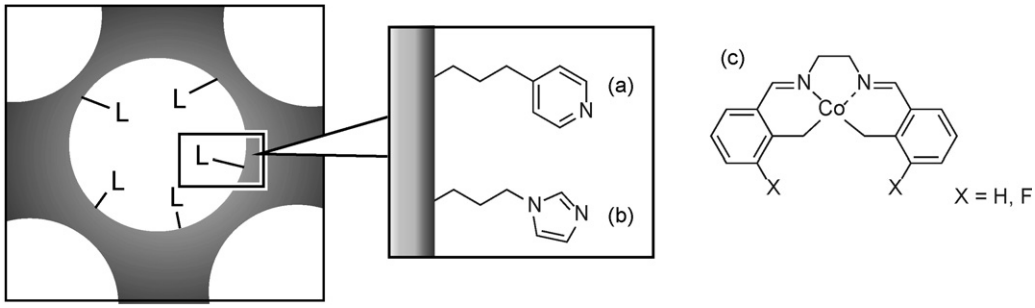

Fig. 7. Metal coordination sites immobilized in mesoporous silica.

silica has been achieved through coordination of the cobalt to pyridine or imidazole groups covalently attached to the silica matrix (Fig. 7) [100]. The imidazole group appears to be a slightly better coordinating group and coordination of Co-fluomine was achieved by using the corresponding materials with imidazole groups. The capacity for O_2 binding of materials containing Co-fluomine was evaluated by static volumetric gas uptake measurements at room temperature. The experimental data indicated that a superoxide complex was formed when tie immobilized Schiff base cobalt(II) complex was exposed to dioxygen and that the dioxygen binding capacity of the materials increased with the proximity of the cobalt centers within the pores. These features suggest the formation of a μ-superoxo complex at the pentacoordinated Co-fluomine incorporated within the mesostructured hybrid materials.

Materials such as mesoporous carbon are hydrophobic and adsorption of functional materials based on such interactions can be conducted effectively. Hu and coworkers investigated adsorption of fullerenes, C_{60} and C_{70}, on four adsorbents including alumina, silica gel, activated carbon, and ordered mesoporous carbon (CMK-3) using a batch system [101]. Fullerenes are considered to have many potential applications, such as in superconductors, industrial catalysis, and perhaps as antiviral agents [102]. While alumina and silica gel have small adsorption capacity for fullerenes, both CMK-3 and activated carbon can adsorb fullerenes. In particular, the adsorption capacity of CMK-3 is 4 times higher than that of the activated carbon. In addition, C_{70} is more strongly adsorbed on CMK-3 than C_{60}. Inumaru et al. reported interesting results from design of a nanospace for better selectivity in adsorption of organic compounds [103,104]. Tunability in the length of alkyl chain grafted onto the mesopore surface is very influential with respect to adsorption performance of alkylated compounds. Nonylphenol, an endocrine disrupter, is efficiently removed by adsorption onto *n*-octyl grafted MCM-41, while adsorption of *tert*-amylphenol is weak and that of phenol is undetectable. A large volume of highly hydrophobic nanospaces surrounded by ionic inorganic walls is important for efficient adsorption of alkyl phenols. Molecules that fit well the inorganic–organic nanostructure are preferentially adsorbed. Thus, the adsorbent can achieve high molecular adsorption selectivity. A strategy using co-operative function between organic and inorganic moieties heralds the development of more sophisticated nanomaterials. Mesoporous materials have been used also for gas permeation control as demonstrated by Kim and Marand [105]. Mesoporous MCM-48 silica was synthesized by a templating method and mixed with polysulfone to fabricate mixed matrix membranes. The high surface coverage of silanol groups on MCM-48 provide good interaction with the polysulfone matrix while helium permeation data and SEM images of the resulting MCM-48/polysulfone hybrid membranes suggest that MCM-48 silicate particles adhere well to polysulfone and that the membranes prepared were defect free. The continuous pathways present in the polymer matrix with the high loading of MCM-48 silica allowed the gas molecules to diffuse solely through the molecular sieve phase resulting in high gas permeation performance.

2.2. Sensing

Mesoporous nanospaces provide a confined environment where cooperative functionality of two species can be accommodated. Combining binding ability with sensing function for target molecules leads to unique sensor materials. Li and coworkers grafted 1,10-phenathroline onto mesoporous silica as a second ligand for the $Ru(bpy)_2Cl_2$ (bpy = 2,2′-bipyridyl) complex resulting in $[Ru(bpy)_2phen]^{2+}$ groups immobilized at the silicate backbone (Fig. 8A(a)) [106]. The mesoporous structures were obtained as bulk xerogels and spin-coated thin films that provided superior optical oxygen sensors with homogeneous distribution and improved sensitivity. This improvement in oxygen sensitivity is attributed to the increased diffusivity of oxygen in the uniform and nearly parallel porous matrix. Zhang et al. similarly proposed luminescent oxygen sensing materials based on two Pt(II)-porphyrin complexes: platinum meso-tetrakis(4-*N*-methylpyridyl)porphyrin ($PtTMPyP^{4+}$, see Fig. 8A(b)) [107]. The Pt(II)-porphyrin/MCM-41 assembly materials were prepared through simple electrostatic adsorption. Upon increasing oxygen concentration, the emission peak of the Pt(II)-porphyrin/MCM-41 assembly remained at 668 nm and the emission intensity rapidly decreased. The relative luminescent intensities of the sample (20 mg g^{-1}) decreased by 98.2%, upon variation of the atmosphere from pure nitrogen to pure oxygen.

The use of a mesoporous silica as a support for grafting chromophores also opens new opportunities for efficient optical sensors of heavy metals. Palomares et al. investigated the selectivity and sensitivity of two colorimetric sensors based on the ruthenium complexes N719 [bis(2,2′-bipyridyl-4,4′-dicarboxylate)ruthenium(II) bis(tetrabutylammonium)

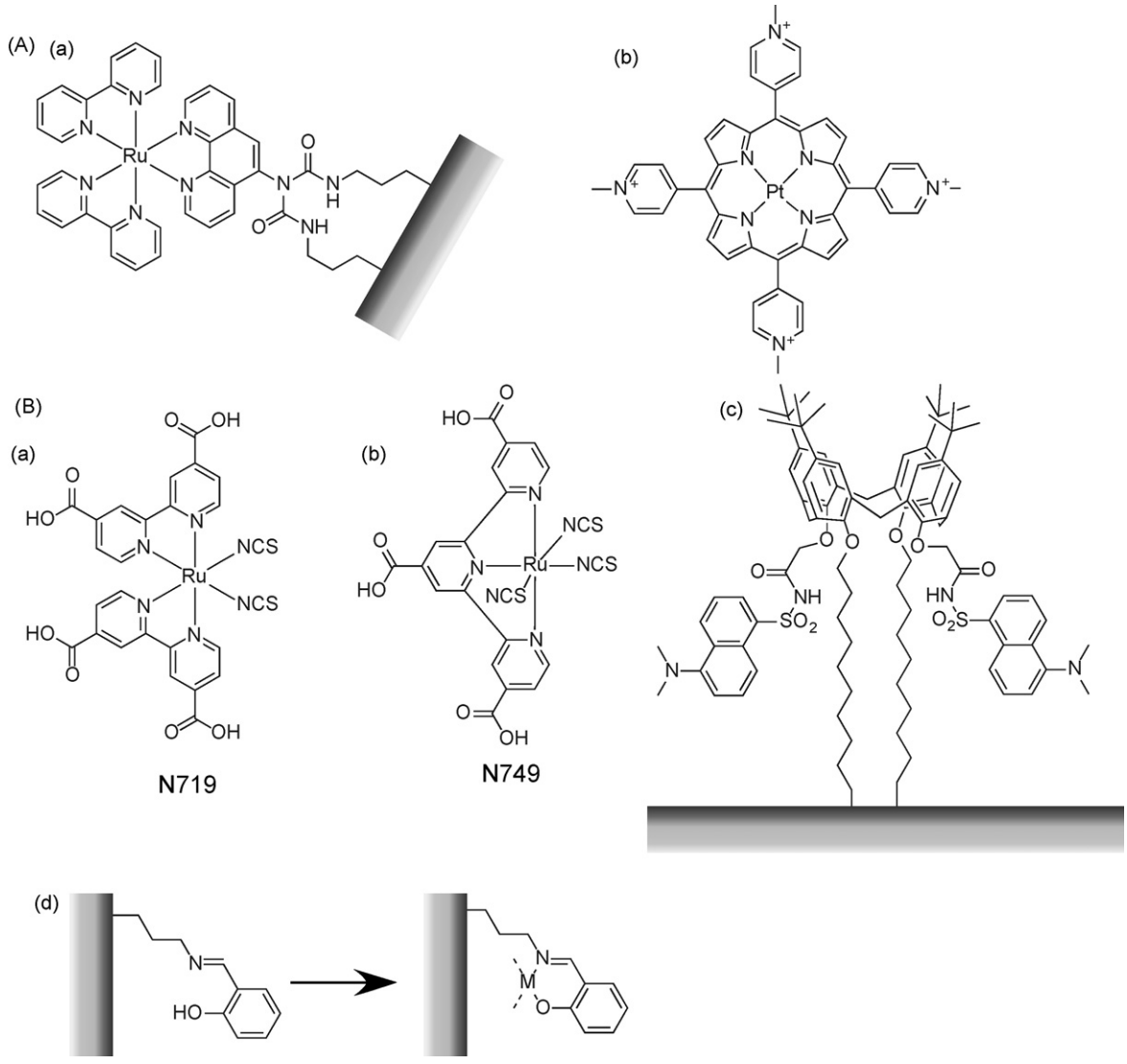

Fig. 8. (A) Oxygen sensing site immobilized on mesopore. (B) Binding sites for optical sensing.

bis(thiocyanate)] and N749 [(2,2′:6′,2″-terpyridine-4,4′,4′-tricarboxylate)ruthenium(II) tris(tetrabutylammonium) tris-(isothiocyanate)] that had been immobilized in mesopore nanospace (Fig. 8B(a) and (b), respectively) [108]. Hg(II) ions can coordinate reversibly to the sulfur atom of the NCS groups while the sensor molecules can be adsorbed onto high-surface-area mesoporous metal oxide films, allowing reversible heterogeneous sensing of mercury ions in aqueous solution. The interaction between Hg(II) ions and the NCS groups of the ruthenium dyes N719 and N749 is responsible for the color change of the corresponding dye. Interestingly, the interaction is selective for Hg(II) even in the presence of much higher concentrations of other potentially competing metal cations such as Pb(II), Cd(II), Zn(II), or Fe(II). The limit of quantification of the systems using UV–vis spectroscopy in homogeneous aqueous solutions is estimated to be ca. 20 ppb for N719 and ca. 150 ppb for N749. Nazeeruddin, Grätzel, and coworkers used modified dye, *cis*-dithiocyanatobis-2,2′-bipyridine-4,4′-(COOH)2-4,4′-tridecyl-2,2′-bipyridineruthenium(II), ([Ru(dcbpyH)(tdbpy)$(NCS)_2$]; N621) and bistetrabutylammonium *cis*-dithiocyanatobis-2,2′-bipyridine-4-COOH,4′-COO^--ruthenium(II), ($(Bu4N)_2$[Ru(dcbpyH)$_2(NCS)_2$]; N719) containing hydrophobic alkyl tails or hydrophobic counterions, respectively, in order to suppress leaching of the sensing sites from mesoporous structures [109]. They achieved fully reversible optical sensing of Hg(II) ions with extraordinary selectivity and sensitivity using nanocrystalline TiO_2 films decorated with these functionalized ruthenium sensitizers. Hg(II) ions coordinate reversibly to the Ru(II) sensitizers, inducing a color change and increasing the phosphorescence intensity significantly. Leray and coworkers reported preparation of a calixarene bearing two dansyl fluorophores grafted onto a large pore mesoporous silica SBA-15 material through two long alkyl chains containing triethoxysilane groups (Fig. 8B(c)), in order to establish optical sensing of Hg(II) ions in water [110]. This functionalized material is able to reversibly detect Hg(II) ions with a response time of a few seconds and a detection limit of 3.3×10^{-7} M in water. Furthermore, this system offers a

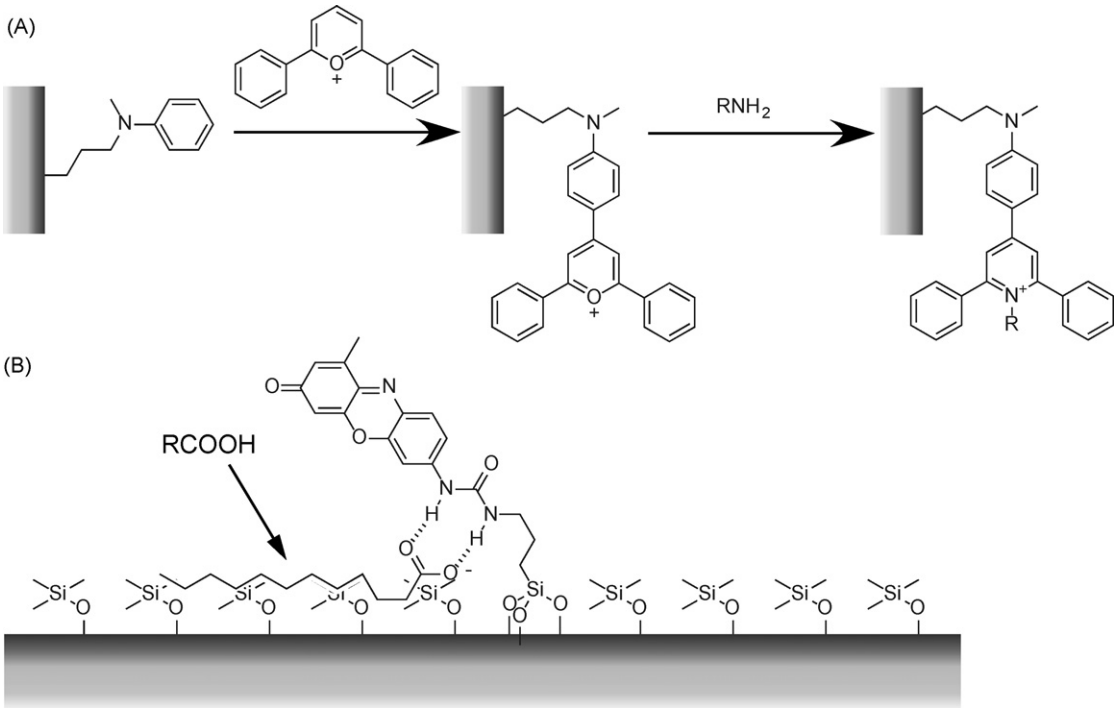

Fig. 9. (A) Sensing site for amine guest. (B) Sensing site for fatty acid. Reprinted with permission from [114], ©2005, American Chemical Society.

high selectivity over several interfering cations (Na^+, K^+, Ca^{2+}, Cu^{2+}, Cd^{2+} and Pb^{2+}). Wang and coworkers grafted luminescent Schiff-base groups on the surface of mesoporous material MCM-48 and employed it to sense metal ions (Fig. 8(d)) [111]. The first step involved the treatment of the MCM-48 surface with 3-aminopropyl-(trimethoxy)silane followed by condensation between amine groups and 2-hydroxybenzaldehyde. Treatment of suspensions of the Schiff-base-containing MCM-48 with Zn(II) ions in aqueous solution resulted in solid yellow materials that fluorescence strongly. The fluorescence of the prepared MCM-48 solid with Schiff-base groups could be quenched completely by Cu(II) ions, was and so proved suitable for sensing Cu(II) ions in aqueous media. Cu(II) could quench completely the emission of the parent material even in the presence of equimolecular Zn(II), Co(II), Ca(II), Pb(II), Ni(II), Mn(II), or Cd(II) ions.

Target analytes are not limited to gaseous substances or metal ions. García-Acosta et al. reported the rational development of sensory materials for the chromo- and fluorogenic detection of biogenic amines in complex liquid samples [112,113]. The probe molecule is a reactive pyrylium chromophore that is anchored into the inner hydrophobic pores of a mesoporous siliceous support (Fig. 9A). Although fatty amines are biologically important, they are often silent in some kinds of chromo-fluorogenie tests. The prepared mesoporous materials realized considerable color changes upon binding to fatty amines through formation of the corresponding pyridinium derivatives. Use of mesoporous materials as chromophore supports leads to size discrimination of the guest amines. Amines with a medium-sized alkyl or alkyl-aryl end group exhibit a much faster response than the fatty amines. Rurack and coworkers immobilized a spacer-substituted 7-ureaphenoxazin-3-one as the signaling moiety onto a mesoporous trimethylsilylated MCM-41 type mesoporous silica material for optical sensing of fatty acids (Fig. 9B) [114]. A fatty carboxylate-induced chromogenic reaction accompanied by a strong enhancement of fluorescence emission in the 600 nm range clearly shows that optimization of the signaling unit is equally important for selectivity in powerful sensing devices. Fig. 9B can be rationalized as the sensing of the long-chain tail by the hydrophobic walls, so that the polar head groups stick to the outside. In this microscopic boundary layer of reduced water content, the hydrogen bond-mediated binding reaction between the probe's receptor group and the carboxylate group is then facilitated and leads to signal generation. In addition to these examples, several reseraches on sensing functions using mesoporous nanospaces have been reported [115–118].

2.3. Catalysis

Mesoporous materials have been used as supports for catalysts mostly because of their extremely large surface areas. When compared with zeolite materials, which contain narrow pores, mesoporous materials have the advantage of a more facile diffusion of material into the pores. However, the large size of mesopores compared to the molecular dimensions of reactants is somewhat disadvantageous for control of substrate orientation within the pores. To alleviate this problem, specific incorporation of larger catalytic sites such as designated organic groups, metal-coordination complexes, and nanoparticles into the mesopore environment. Mesoporous nanospaces have been used for specific catalysis as shown below.

Lin and coworkers introduced the principle for synthesis of a class of bifunctionalized mesoporous silica nanosphere materials, where one common functional group (primary group)

serves as a catalyst and the other functionality (secondary group) delivers different noncovalent interactions to reagents and thereby controls the reaction selectivity (Fig. 10A) [119]. By tuning the hydrophilic nature of the secondary group, the selectivity of the nitroaldol (Henry) reaction between competing benzaldehydes and nitromethane catalysed by the 3-[2-(2-aminoethylamino)ethylamino]propyl group can be controlled. The monofunctionalized and hydrophilic bifunctionalized catalysts did not show any reaction selectivity for all three combinations of the reactants. In contrast, an increase of reaction selectivity toward the nonpolar and more hydrophobic alkoxybenzaldehyde reactants was clearly observed. The results obtained suggest that the hydrophobic secondary groups play a significant role in preferential penetration of the more hydrophobic reactants into the mesopores and subsequent reaction at the 3-[2-(2-aminoethylamino)ethylamino]propyl functionality. Lin and coworkers also reported catalytic activity of a 4-(dialkylamino)pyridine-functionalized mesoporous silica nanosphere material for various reactions: Baylis-Hillman, acylation, and silylation reactions (Fig. 10B) [120]. For example, the functionalized mesoporous silica material showed an excellent catalytic performance during the Baylis-Hillman reaction of aryl aldehydes and various unsaturated ketones. Only a catalytic amount of the functionalized silica was required for the complete conversion of cyclic and aliphatic enones to the corresponding Baylis-Hillman products.

Matsuoka and coworkers studied incorporation of arenetricarbonyl complexes [–phM(CO)$_3$–] (ph = C_6H_4 and M = Cr, Mo) within the organosilica framework of phenylene (–C_6H_4–)-bridged mesoporous materials by a simple chemical vapor deposition method (Fig. 11A(a)) [121]. A high thermal stability of the hybrid materials was also achieved. This novel mesoporous material can be utilized in the development of unique heterogeneous catalysts since arenetricarbonyl complexes exhibit effective catalytic activity for reactions such as the hydrogenation of polyunsaturates into *cis*-unsaturated products. The immobilized complex can undergo various transformations of their arene moieties because of the large electron-withdrawing ability and stereocontrolling effect of the Cr(CO)$_3$ moieties. Dufand et al. reported the development of new methodologies for the preparation of rhodium organophosphine complex hybrid materials in which the organometallic complexes are integrated within the pore walls of highly ordered mesostructured silicates (Fig. 11A(b)) [122]. The catalytic activity of several hybrid materials for hydrogenation was evaluated using substrates of varying steric encumbrance and compared to the activity of a homogeneous catalyst, [RhCl(PPh$_3$)$_3$]. For styrene hydrogenation, the activity is in the same range as that observed for the homogeneous complex. In addition, greater catalytic activity was observed for the more hindered double bonds of cyclohexene and crotonaldehyde and this activity was undiminished over several cycles. Freire and coworkers used the (3-aminopropyl)triethoxysilane anchored Cu(II) acetylacetonate coordination complex in hexagonal mesoporous silica materials [123]. The anchoring process was performed using Schiff condensation with the free amine group, which were covalentry attached to the silica surface with the carbonyl groups of the Cu(II)-coordinating acetylacetonate ligand, as depicted in Fig. 11B. The materials obtained were tested in the aziridination of styrene, using PhI = NTs as nitrogen source and acetonitrile as solvent, at room temperature. The styrene conversion and total turnover number of the heterogeneous phase reaction were higher than those of the same reaction catalyzed in homogeneous phase by [Cu(acac)$_2$].

Metal-doped mesoporous silica materials have been used widely for catalytic purposes [124–133]. Selected recent examples are show below. Nakamura and Frei, used Cr(III) doped mesoporous silica for visible light-induced water oxidation as demonstrated at a polynuclear catalyst coupled directly to a molecular charge-transfer moiety within a nanoporous solid [134]. Crudden et al. synthesized Pd-encapsulated SBA-15 mesoporous silica with the aid of mercaptopropyl groups, which catalyzed the Mizoroki-Heck and Suzuki-Miyaura reactions, without leaching Pd into solution [135]. Antonelli and coworkers demonstrated that mesoporous tantalum oxide doped with Ru(II) and Ba(II) ions is an active catalyst for the conversion of N_2 and H_2 into ammonia [136]. Ma and coworkers proposed that coating of mesoporous silica with a layer of a molecule containing functionalities with labile coordinating ability would protect a metal complex under unfavorable conditions [137]. They realized this concept by producing a highly active mesoporous silica-supported palladium catalyst upon coating with poly(ethylene glycol), which possessed high activity in Suzuki coupling reactions in water. It is well known that Pd(PPh$_3$)$_4$ is unstable, losing catalytic activity upon exposure to air, but the supported catalyst in mesoporous silica was still effective even after exposure to air for 6 weeks. Reactions could also be conducted in the open air without any obvious loss of activity. The catalyst in water could be reused without any obvious loss of the activity, and leaching of the Pd into the organic layer after the reaction was not observed. Andersson et al. prepared thin films of ordered mesoporous TiO_2 anatase using a dip-coating procedure and silver nanoparticles were introduced into the mesopores using wet impregnation followed by heat treatment [138]. Their photocatalytic activity for oxidation of stearic acid was investigated.

Mesoporous nanospaces are known to provide an appropriate environment for size-controlled materials that often have nanometer-scale dimensions and show quantum effects. Zhao and coworkers developed a flexible approach for fabrication of uniform nanocrystals and nanowires of the semiconductor PbS inside the nanospaces of mesoporous silica SBA-15 [139]. A massive blue shift observed in photoluminescence spectra clearly indicates quantum size effects in the PbS nanocrystals and nanowires. Larionova and coworkers prepared size-controlled Mn_3O_4 nanoparticles by thermal decomposition of a precursor [$Mn_{12}O_{12}(C_2H_5COO)_{16}(H_2O)_3$] anchored to a hybrid silica containing an appropriate functional group (Fig. 12) [140]. Chemical anchoring of the magnetic cluster [$Mn_{12}O_{12}(C_2H_5COO)_{16}(H_2O)_3$] to an ordered hybrid silica matrix containing –COOH functionalities followed by the intrapore growth of nanosized Mn_3O_4 particles by thermal treatment. A variety of physical characterizations allowed monitoring of the evolution of the materials at each step of the synthesis. The

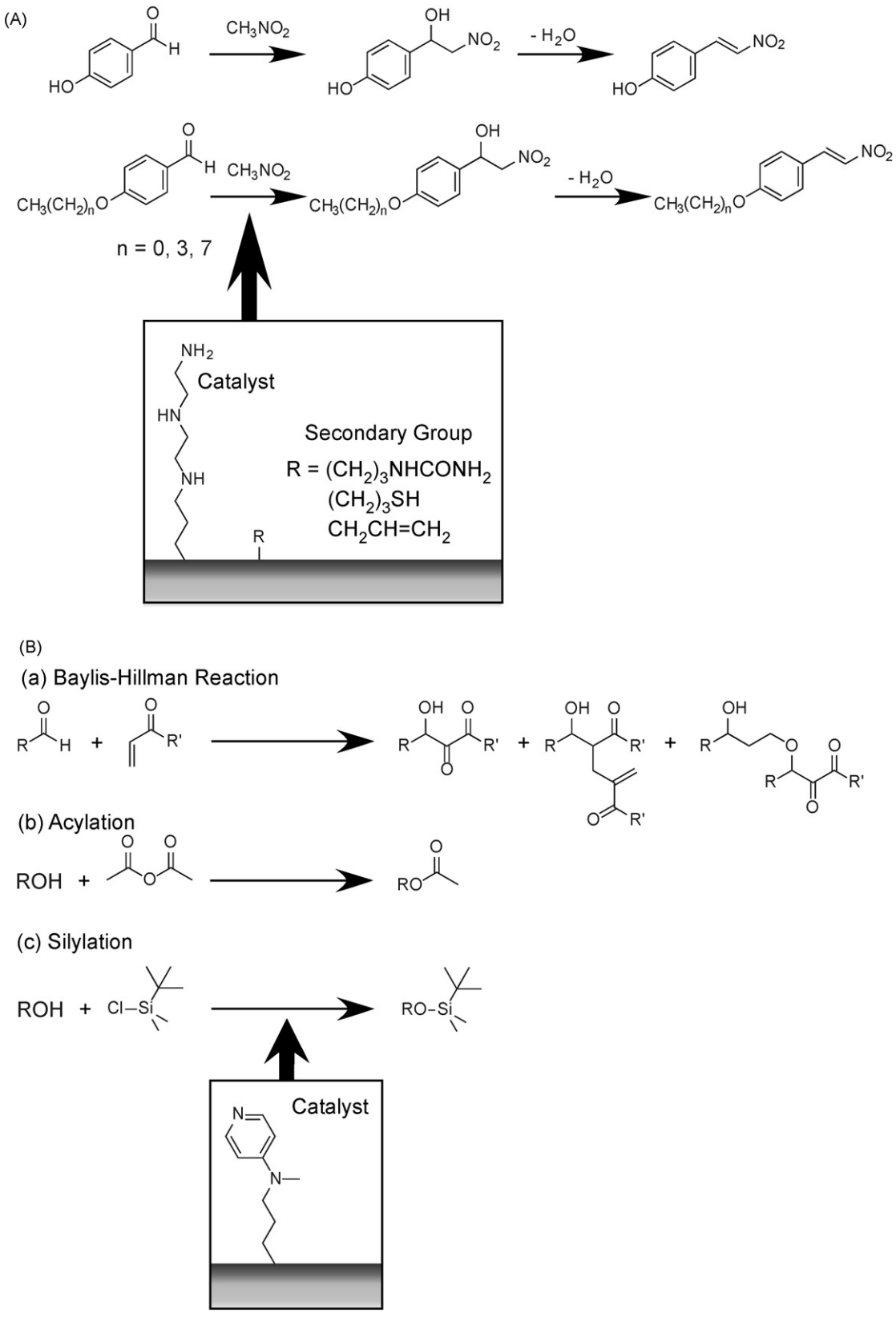

Fig. 10. Organic catalytic sites immobilized on mesoporous silica: (A) poly amine-type catalyst; (B) aminopyridine-type catalyst.

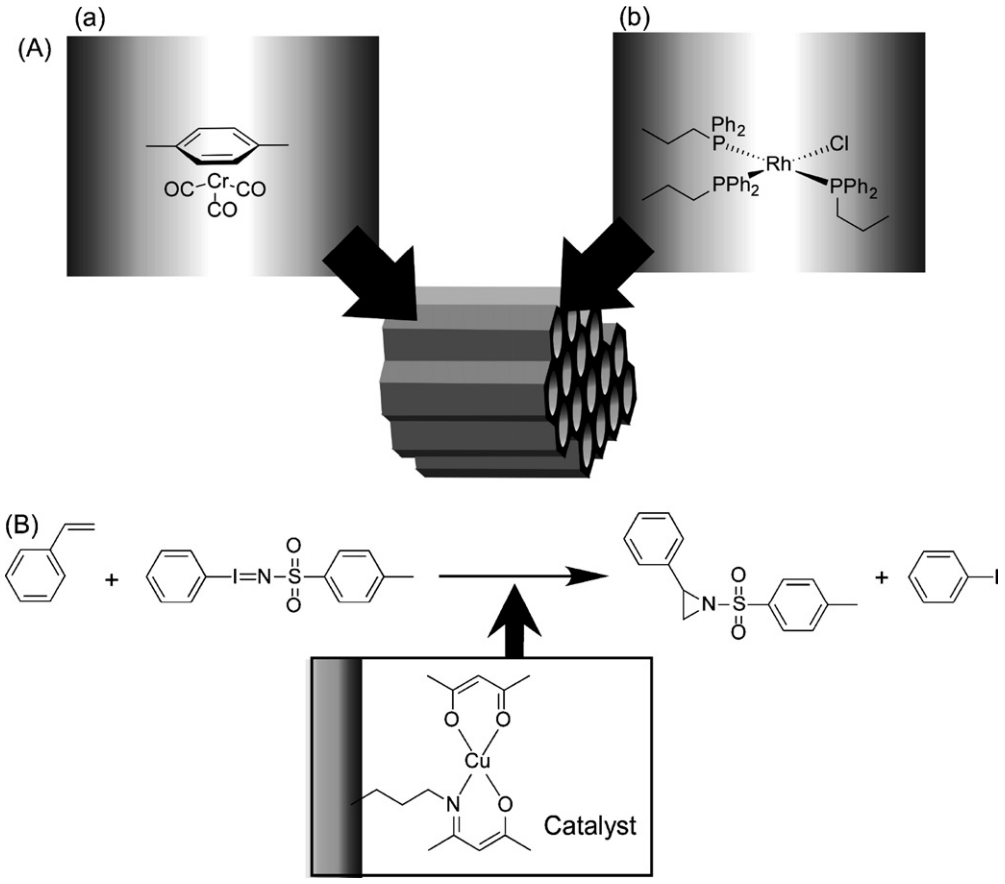

Fig. 11. Metal coordination complex as catalytic sites in mesopore nanospace: (A) (a) Cr complex and (b) Rh complex; (B) Cu complex.

size of Mn_3O_4 nanoparticles was well controlled with a size distribution centered at ca. 8 nm and they were situated exclusively inside the silica matrix. Covalent anchoring of the cluster inside the functionalized silica plays a crucial role in the fabrication of the Mn_3O_4 nanoparticles. The initial dispersion of the bonding sites of the hybrid silica avoids both aggregation and extrusion of the manganese oxide formed and permits the control of the nanoparticle dispersion. Fukuoka et al. synthesized nanowires of platinum and gold with high aspect ratios in one-dimensional channels of ordered mesoporous organosilica [141]. They impregnated using the corresponding metal precursors followed by their reduction to metal nanostructures. Water-saturated hydrogen reduction (wet H_2-reduction) is effective for large-scale synthesis of long nanowires, while dry

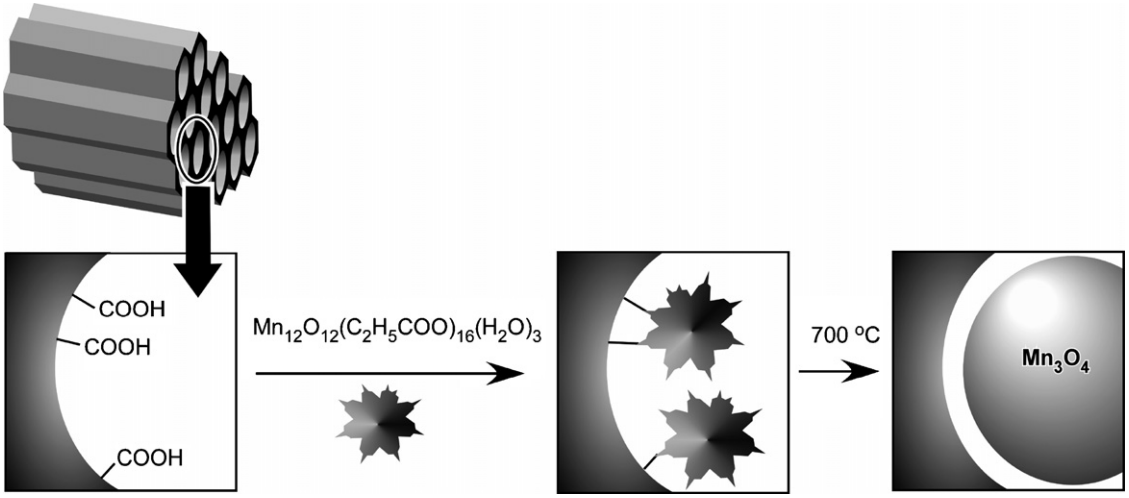

Fig. 12. Formation of Mn_3O_4 nanoparticle from Mn cluster anchored on mesoporous silica. Reprinted with permission from [140], ©2004, Royal Society of Chemistry.

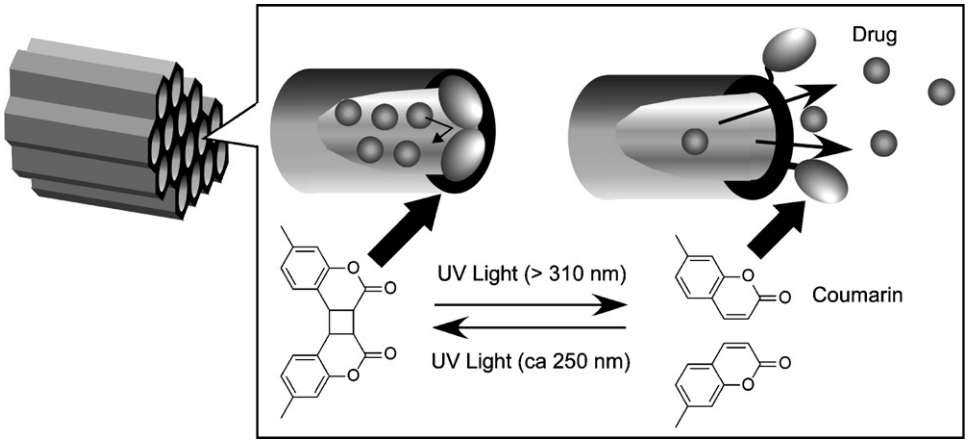

Fig. 13. Controlled release of drugs from coumarin-functionalized mesoporous silica. Reprinted with permission from [145], ©2003, American Chemical Society.

H_2-reduction gives monodispersed metal nanoparticles. Stucky and coworkers reported a general methodology that utilizes confined mesoporous silica as a template for preparation of highly ordered mesostructured nanowires and nanowire arrays [142]. The Ag, Ni, and CU_2O nanowires prepared had the unique features of hierarchical organization, modulated surface morphology, high surface area, and chirality with unprecedented mesostructures including coaxially multilayered helical, and stacked-donut structures. Yang and coworkers synthesized monodisperse platinum nanoparticles of 1.7–7.1 nm diameter by alcoholic reduction methods and incorporated them into mesoporous SBA-15 silica during hydrothermal synthesis [143]. Ethane hydrogenolysis displayed significant sensitivity to the particle size. The observed dependence of rate on particle size is attributed to a higher reactivity of coordinatively unsaturated surface atoms in small particles compared to low-index surface atoms prevalent in large particles.

2.4. Controlled release

Mesoporous materials have considerable pore volumes per weight and well controlled dimensions for the pore inlet. Therefore, these materials are suitable for storage of guests and their controlled release.

In pioneering work, Fujiwara and coworkers achieved photocontrolled regulation of drug storage and release from mesoporous silica (Fig. 13) [144,145]. They prepared MCM-41 mesoporous silica functionalized with photoactive coumarin that was grafted only at the pore outlet. Guest drugs, such as cholestane, were incorporated into the mesopores of template-free silica upon exposure to the guest solution. Irradiation by UV light (>310 nm) causes dimerization of coumarin for trapping of the guest cholestane in the stable form and blocks leaching of the guest from the mesopores. The dimerized coumarin was cleaved upon irradiation with a different wavelength of UV light (∼250 nm) resulting in release of trapped cholestane. Lin and coworkers realized a mesoporous silica-based controlled-release delivery system using colloid capping (Fig. 14) [146]. Their stimuli-responsive system consists of a 2-(propyldisulfanyl)ethylamine functionalized mesoporous silica nanosphere material with an average particle size of 200.0 nm and an average pore diameter of 2.3 nm. The mesopores were also used to store various drug molecules or neurotransmitters, such as vancomycin and adenosine triphosphate (ATP). The entrance of the mesopores of the drug/neurotransmitter-loaded mesoporous material was then capped *in situ* by allowing the pore surface-bound 2-(propyldisulfanyl)ethylamine functional groups to covalently capture the water-soluble mercaptoacetic acid-derivatized CdS nanocrystals. The resulting disulfide linkages could be chemically cleaved using various reducing

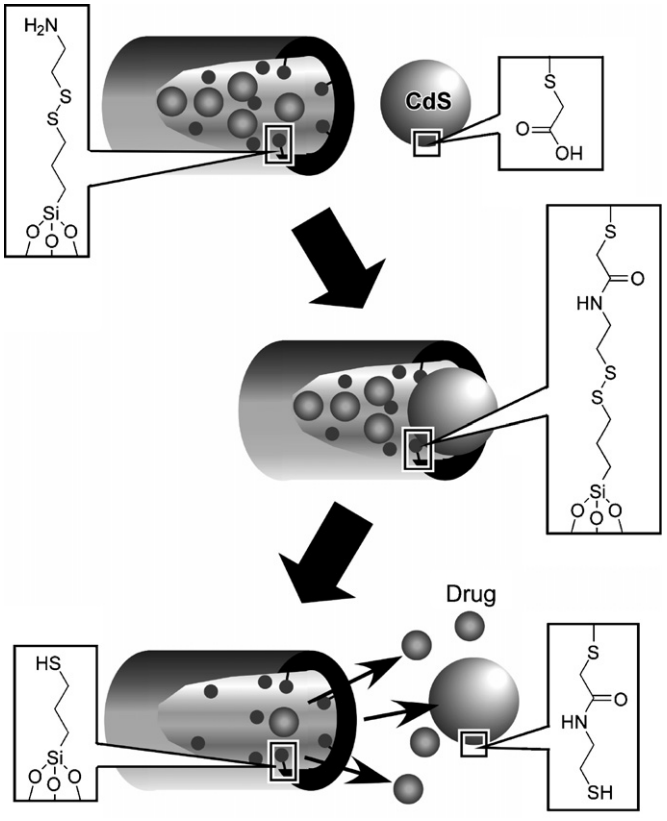

Fig. 14. Controlled release of drugs from mesoporous silica by colloidal capping. Reprinted with permission from [146], ©2003, American Chemical Society.

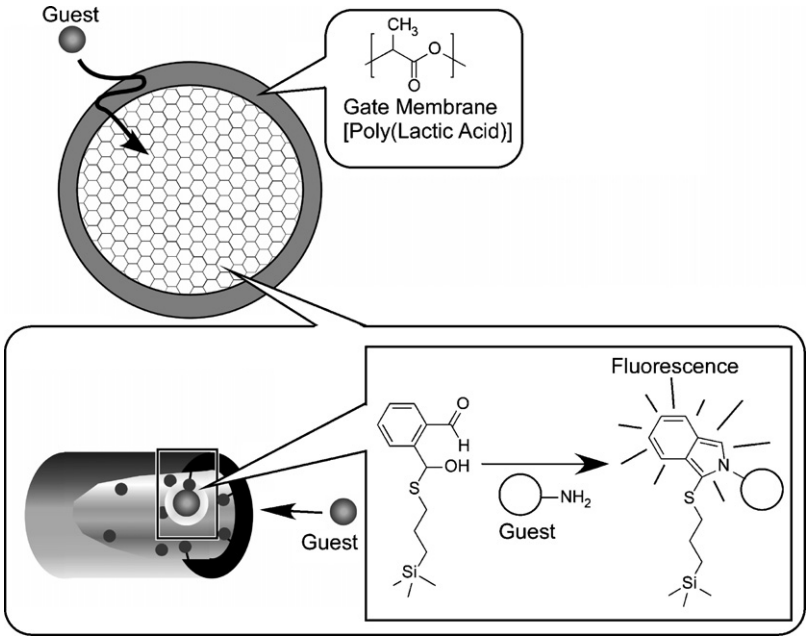

Fig. 15. Gate-controlled molecular recognition with mesoporous silica structure. Reprinted with permission from [147], ©2004, American Chemical Society.

agents, such as dithiothreitol or mercaptoethanol. Thus, stimuli-responsive release was realized while the system's *in vitro* biocompatibility with neuroglial cells (astrocytes) was also confirmed. Lin and coworkers also demonstrated gate-controlled molecular recognition by selective functionalization of external and internal surfaces of mesoporous silicates [147]. In the first step, thiol-modified MCM-41 type mesoporous silica nanosphere silica was synthesized using a co-condensation route. Before removal of the surfactant template, epoxyhexyl groups were grafted selectively at the external surface of the mesoporous silica. Epoxy groups were then converted to dthydroxyhexyl group and L-lactide was polymerized at the external surface followed by the immobilization of *o*-phthalic hemithioacetal group at the internal thiol group (Fig. 15). The *o*-phthalic hemithioacetal can operate as an optical sensor by fluorescing upon reaction with amines such as dopamine (aneurotransmitters), tyrosine, or glutaric acid. The polylactate layer at the exterior plays the role of gatekeeper, resulting in selectivity of detection for the neurotransmitters. Lin and coworkers synthesized a series of room temperature ionic liquid containing mesoporous silica nanoparticle materials with various particle morphologies, including spheres, ellipsoids, rods, and tubes [148]. They also investigated the controlled release profiles of the materials by utilizing ionic liquids as antibacterial agents against the Gram negative microbe *Escherichia coli K12*. Antibacterial activity was dependent on the rate of diffusional release of the pore-encapsulated ionic liquid, which was governed by the particle and pore morphology of the mesoporous silica nanospheres. A novel gene transfection system using mesoporous materials was demonstrated by Lin and coworkers [149]. In their report, a second generation poly(amidoamine) dendrimer was covalently attached to the surface of MCM-41-type mesoporous silica nanospheres and this dendrimer-capped material was complexed with a plasmid DNA (pEGFPCl) coding for an enhanced green fluorescence protein. Gene transfection efficacy, uptake mechanism, biocompatibility with neural glia (astrocytes), human cervical cancer (HeLa), and Chinese hamster ovarian (CHO) cells were all investigated. The mesoporous structure allows membrane-impermeable molecules, such as drugs or fluorescent dyes, to be encapsulated inside the mesoporous nanospaces. The system introduces the possibility of a universal transmembrane carrier for intracellular drug delivery and imaging applications. The same research group has very recently investigated drug uptake by mesoporous silicates to assess their potential as controlled delivery materials [150]. The uptake of MCM-41-type mesoporous silica nanoparticles by HeLa cells can be regulated by varying surface functionalization. The results reported indicate that these surface functionalities also affect the ability of mesoporous silica to escape endosomal entrapment, which is a key factor in designing effective intracellular delivery vehicles.

Martínez-Máñez and coworkers used an MCM-41 mesoporous solid support functionalized at its external surface with polyamines for controlled entrapment and release of guest anions [151]. At acidic pH, the amines are fully protonated, the polyamine gate is closed, and no $[Ru(bipy)_3]^{2+}$ guest is released. This functional nanoscopic pore blockage is related to the repulsion between protonated polyamines, which are mutually repelled towards the pore openings, and the cationic $[Ru(bipy)_3]^{2+}$ guest. In contrast, at neutral and slightly basic pH, the attached polyamines are only partially protonated, the effects contributing to pore blockage are much less pronounced, and there is a massive delivery of the $[Ru(bipy)_3]^{2+}$ guest from the pores to the solution. The ability of the materials to deliver the $[Ru(bipy)_3]^{2+}$ guest at neutral pH was also studied in the presence of fluoride, chloride, bromide, iodide, nitrate, phosphate, sulfate, acetate, and carbonate anions without notably affecting the delivery process. Even at concentrations of up to

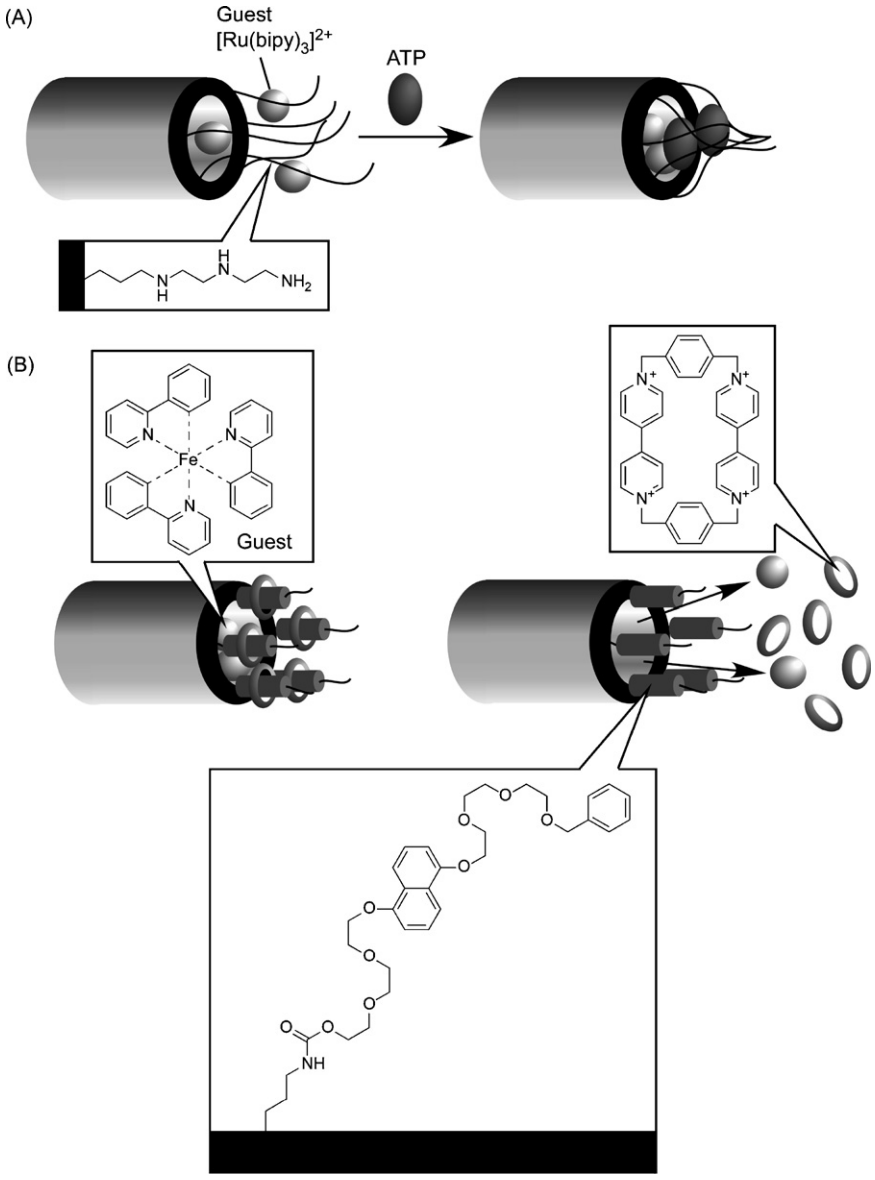

Fig. 16. Controlled release and storage of drugs from mesopore with pore-blocking reagents: (A) ATP blocking; (B) rotaxane blocking. Reprinted with permission from [152], ©2004, American Chemical Society.

0.01 M of anions, there was no significant influence on the dye delivery process and in all cases, virtually identical dye release kinetics were found. In contrast, upon adding aqueous solutions of adenosine triphosphate (ATP) and adenosine diphosphate (ADP), the pores of the mesoporous materials were blocked (Fig. 16A). The chromogenic response of the designed materials was related to the ability of the protonated polyamines to strongly coordinate nucleotides. The extent of this coordination was good enough at neutral pH to block the pores and the strength of the interaction was enhanced by a preorganization effect that arises from grafting the polyamine moieties onto the inorganic supports. Pore blockage is observed for anions that form strong complexes with polyamines (ATP > ADP > GMP). Stoddart and coworkers reported the tethering of pseudorotaxanes as gates at the entrances of the cylindrical pores in mesostructured silica creating nanovalves capable of trapping luminescent molecules and able to release them on demand (Fig. 16B) [152]. The [2]pseudorotaxane was employed as a gatekeeper in the form of a tethered 1,5-dioxynaphthalene-containing derivative, acting as the gatepost, and cyclobis(paraquat-*p*-phenylene), which recognizes dioxynaphthalene units because of a cooperative array of noncovalent interactions, serving as the gate that controls access in and out of the nanopores. An external reducing reagent ($NaCNBH_3$) opens the nanovalve and allows the release of the luminescent molecules. The same research group also realized a reversibly operating nanovalve that can be toggled on and off using redox chemistry [153]. It traps and releases molecules from the maze of nanoscopic passageways in silica by controlling the operation of redox-activated bistable [2]rotaxane molecules tethered at the openings of nanopores at the exits of the nanoscale reservoir. The rotaxane-modified MCM-41 constitutes a class of organic–inorganic hybrid nanoparticle

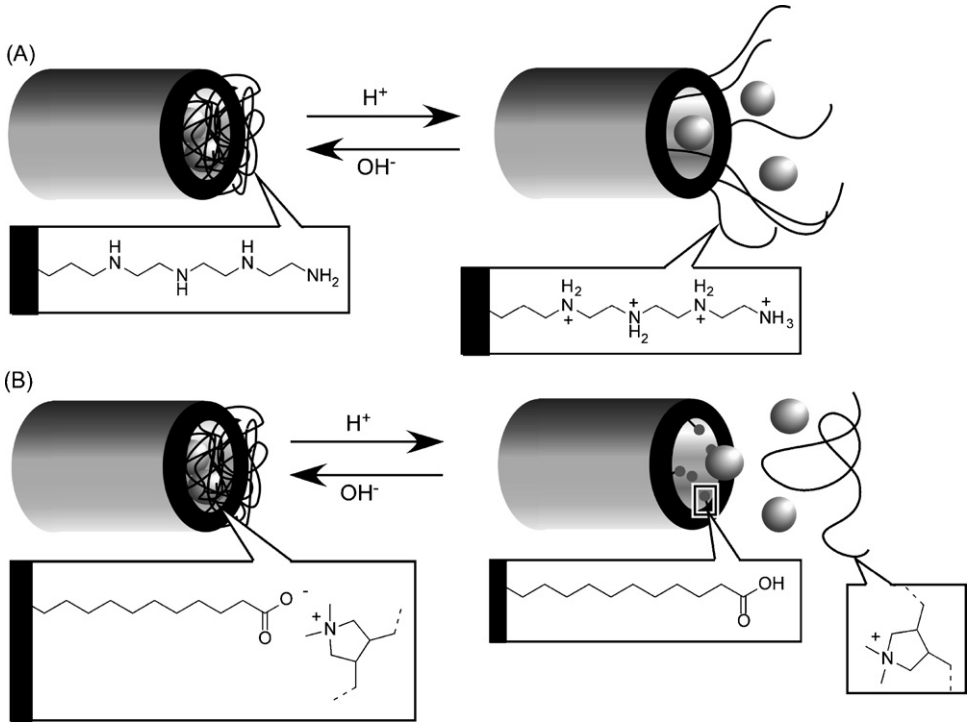

Fig. 17. pH-controlled opening-closure of functionalized mesopores: (A) with amine protonation; (B) with forming polyion complex. Reprinted with permission from [154,155], ©2004 and ©2005, American Chemical Society.

that utilizes the mechanical movement within a mechanically interlocked molecule to control trapping and release of guest molecules. This operational valve is a true molecular machine consisting of a solid framework with movable parts to accomplish a reversible operation.

Among potential external stimuli, solution pH is one generally applicable factors. Martínez-Máñez and coworkers demonstrated an ionically controlled molecular gate using functionalized mesoporous materials with pH-responsive groups at the pore outlets [154]. Ion-sensitive groups were introduced to mesoporous silica by grafting $(EtO)_3Si–CH_2CH_2CH_2(NHCH_2CH_2)_2NH_2$ prior to template removal, leading to a preferential anchoring of the amino groups at the external surface. Removal of the template resulted in a locally functionalized mesoporous silica material. The pH-controlled "open-close" mechanism could arise from hydrogen-bonding interactions between amines (open-gate) and Coulombic repulsion between ammonium groups (closed-gate) (Fig. 17A). Additionally, a synergic anion-controlled outcome could result from formation of complexes between the protonated amines and a certain anion. For example, a larger "shielding effect" controlling the access to the pores is expected in the presence of bulky anions capable of displaying strong interactions with protonated amines than in the presence of small anions poorly coordinated by polyamines. Xiao and coworkers also reported a pH-responsive carrier system based on carboxylic acid modified SBA-15 silica rods and poly (dimethyldiallylammonium chloride) (PDDA) for storage and release of drug molecules from pore voids [155]. Polycations (PDDA) absorbed to anionic SBA-15 by oppositely charged ionic interaction act as closed gates for storage of drugs in the mesopores and upon transformation of ionized carboxylic acid species into protonated groups by lowering of the pH value, polycations are separated from the surface of modified SBA-15, leading to opening of the gates for release of drugs from the mesopores.

Oral administration usually has the drawback of very low absorption of drugs into the body and it is not appropriate for some kinds of drug that need rather high local concentrations. Bisphosphonates, analogues of pyrophosphates, are a family of drugs that inhibit bone resorption by osteoclasts and are resistant to hydrolysis. However, they show a poor intestinal absorption of typically less than 1%. The confinement of bisphosphonates in the pores of silica-based ordered mesoporous materials for a local and controlled drug delivery would be useful for repairing bone defects and would presumably show a better adsorption behavior. Vallet-Regí and coworkers used two types of hexagonally ordered mesoporous materials, MCM-41 and SBA-15 as matrices for alendronate (bisphosphonate) adsorption and release [156]. In that case the drug uptake rate can be increased from 1% to 40% of bisphosphonate. The amount and delivery rate of bisphosphonate can be modulated by organic modification on the surface of the pore walls. When amine groups are covalently grafted to the silanol groups at the pore surfaces, the bisphosphonate adsorption is increased almost three-fold, with a subsequent intensification of the drug dosage in the required area. The same research group also reported controlled delivery of macrolide-type antibiotics using SBA-15 [157]. The SBA-15 analogue was charged with the macrolide antibiotic erythromycin and release assays were carried out *in vitro*. In relation to this system, it has been observed that the release rate decreases as the popula-

tion of hydrophobic $–CH_2$ moieties in the host increases. Lin and coworkers reported a controlled-release delivery system that is based on MCM-41-type mesoporous silica nanorods capped with superparamagnetic iron oxide nanoparticles which is stimuli-responsive and chemically inert to guest molecules entrapped in the matrix [158]. In their system, the openings of the mesopores were covalently capped in situ through amidation of the 3-(propyldisulfanyl)propionic acid functional groups bound at the pore surface with 3-aminopropyltriethoxysilyl-functionalized superparamagnetic iron oxide (APTS-Fe_3O_4) nanoparticles. The chemically labile disulfide linkages between the mesoporous silica and the Fe_3O_4 nanoparticles could be cleaved with various cell-produced antioxidants and disulfide reducing agents such as dihydrolipoic acid and dithiothreitol, respectively. Hyeon and coworkers report a synthetic procedure for the fabrication of mesoporous silica spheres, which were applied to the uptake and controlled release of drugs [159]. For example, mesoporous silica spheres adsorbed ibuprofen, and the release rate of ibuprofen was controlled by the surface properties of the mesoporous silica spheres. These mesoporous silica spheres are likely to find many biomedical applications. Shul and coworkers synthesized mesoporous Fe/SiO_2 as a carrier for magnetic drug targeting and using the sol–gel route and a chemical reduction method [160]. This mesoporous material could release the drug and can be drawn to the disease site by a magnet, which could be very effective in the case of cancer therapy. Sen et al. reported the template-assisted fabrication of a magnetic mesoporous silica–magnetite nanocomposite and its potential for application in magnetic bioseparations, that is, its ability to bind and elute DNA and extract RNA from bacterial cells [161]. The binding mechanism of DNA on the surface of the nanocomposite is most likely to be due to electrostatic interactions between the negatively charged phosphate backbones of DNA with the positively charged surface of nanoparticles at physiological pH and high salt concentration. A unique example combining molecular assembly techniques and mesoporous materials for controlled release was reported by Wang and Caruso. In their system, enzyme immobilization and encapsulation was accomplished in bimodal mesoporous silica spheres with the aid of layer-by-layer (LbL) assembly [162,163]. The enzymes were immobilized on the mesoporous silica spheres, and a multilayer shell was then assembled on the sphere surface by the LbL electrostatic assembly of oppositely charged species to encapsulate the enzyme. This encapsulation design efficiently suppressed leaching of the enzyme components from the mesoporous materials. Additionally, ca. 98% of the activity of the encapsulated catalase was retained when subjected to proteolysis treatment.

2.5. Biochemical functions

Controlled release from the nanospaces in mesoporous materials is well suited for application to a variety of biological substances. In biological systems, many kinds of confined spaces including enzyme reaction pockets and membrane structures exist in which functional molecules occupy specific orientations in order to perform unusual functions such as highly specific chemical reaction and energy conversion. Therefore, studies on biomaterials within well-defined nanospaces would be very meaningful. Confinement and immobilization of biomolecules within mesoporous nanospaces is a frontier research subject. In this section, several recent examples of immobilization of biomolecules in mesopore nanospaces and their functions are described.

Ariga and coworkers proposed synthesis of a mesoporous silica structure possessing amino acid residues densely packed in its pores (Fig. 18) [164–166]. An amphiphile with condensable alkoxysilane group was used as template and sol–gel reactions together with tetraethyl orthosilicate results in mesoporous silica whose channels are filled with the covalently attached organic groups (alanine residue) of the template. Cleavage and removal of the alkyl tail by selective hydrolysis of the ester at the C-terminal leaves open pores with a surface covalently functionalized by the alanine residue. In this process, the template behaves like a "lizard". Pore formation upon the hydrolysis was also demonstrated by nitrogen adsorption–desorption isotherms. Selective hydrolysis of the template ester was clearly demonstrated by FT-IR measurement of the obtained silica materials. This lizard template method accommodates both the dense functionalization of the pore interior and high accessibility of external guests. Brunel and coworkers demonstrated immobilization of ibuprofen in the mesoporous channels of MCM-41-type mesoporous silica [167]. Ibuprofen was linked to the silica surface through an ester group upon ring opening of 3-glycidoxypropylsilane grafted on the silica. The expected advantages of such a prodrug system are protection of the drug due to its location inside the pores of an inorganic material and its potential release induced by the cleavage of the ester bond by esterases *in vivo*.

Immobilization of large biomolecules such as proteins and DNAs has been investigated by several research groups [163,168–183]. For example, Vinu et al. undertook systematic research on protein adsorption onto mesoporous materials including mesoporous silica [184–188], mesoporous carbon [189–191], and carbon nanocages [68–70] (Fig. 19). The results obtained generally indicate that protein adsorption capability increases as pore volume and/or pore diameter of mesopore materials increases. Charged states of the proteins seriously affect adsorption capacities. Most of the proteins exhibit maximum adsorptions at their isoelectric points where the proteins lose their net charge. In addition, the surface nature of mesoporous materials has an inevitable effect on protein adsorption. Hydrophobic mesoporous carbon often displays superior adsorption capabilities to hydrophilic mesoporous silica. This is because the large pore volume and hydrophobic nature of the carbon nanocage shows superior capability for biomaterials adsorption. As a simple demonstration, adsorption behaviors of lysozyme on the carbon nanocage materials are compared with those of conventional mesoporous carbon. The maximal monolayer adsorption capacity of carbon nanocage is 26.5 $\mu mol\ g^{-1}$, respectively, while that of the representative mesoporous carbon CMK-3 is only 9.8 $\mu mol\ g^{-1}$. Vinu and coworkers have also extended research on adsorption of biomaterials to smaller molecules such as vitamins [192,193] and amino acids [194,195], where the superior adsorption proper-

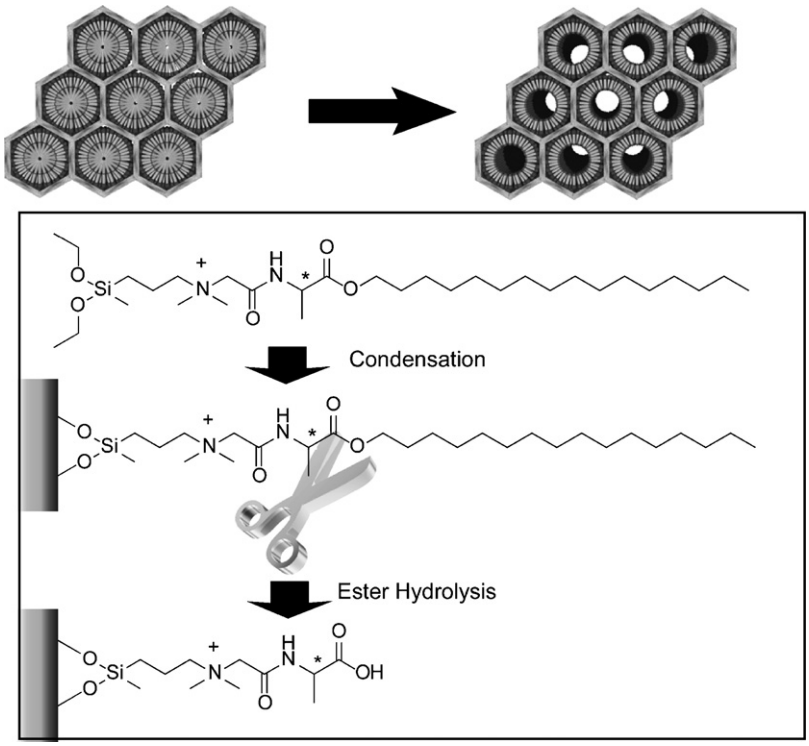

Fig. 18. Lizard template methods for dense immobilization of amino acid residues onto mesopore channel. Reprinted with permission from [165], ©2004, American Chemical Society.

ties of the mesoporous carbon relative to mesoporous silica and activated non-structured carbon is demonstrated. Wall and coworkers investigated the adsorption of an anti-domoic acid single-chain Fv antibody fragment onto a range of mesoporous silicate supports [196].

They are the smallest antibody fragments comprising an intact antigen-binding site and, thus, are capable of retaining the binding properties of their parent antibodies. Their significantly reduced size relative to whole antibodies is an advantage in some applications such as tumor therapy because of improved tumor

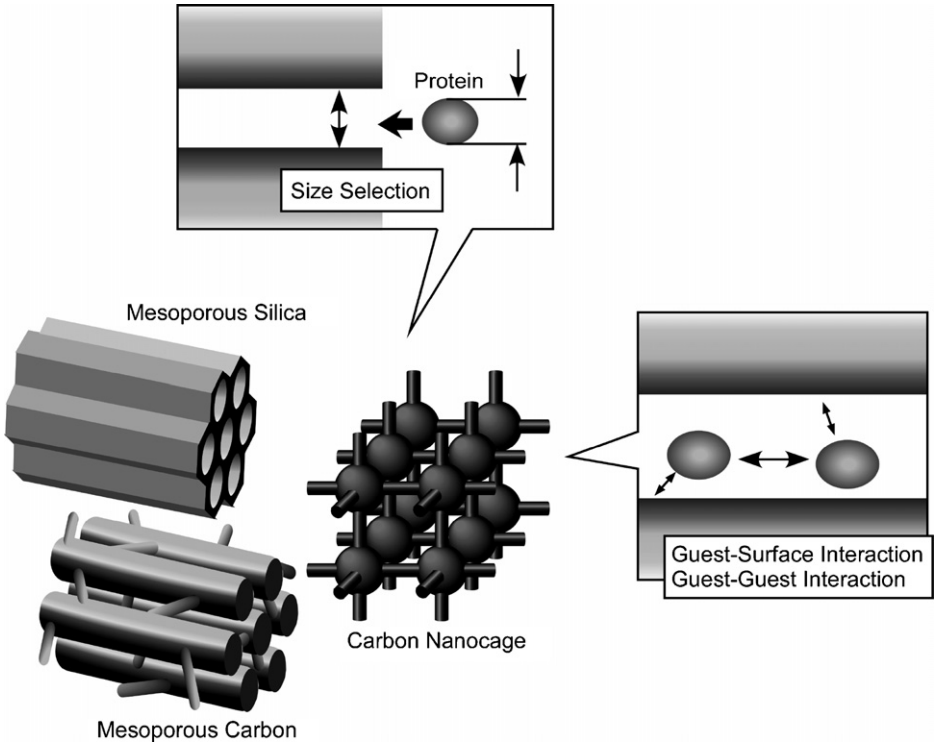

Fig. 19. Factors to influence protein adsorption onto mesoporous materials, mesoporous silica, mesoporous carbon, and carbon nanocage.

penetration and rapid clearance from the body. The immobilized antibody can be bound to its antigen, a naturally occurring neurotoxin produced by shellfish, in a rapidly saturating manner that suggests that the antibody was adsorbed in a multilayer on the mesoporous particles. Solberg and Landry demonstrated adsorption of double-stranded, linear DNA sequences into the pores of spherically shaped mesoporous silica [197]. The mesoporous silica utilized adsorbed a negligible amount of DNA, although introduction of divalent cations such as Mg^{2+} and Ca^{2+} into the mesopores prior to DNA uptake was found to cause a significant enhancement of DNA adsorption. The amount of DNA adsorbed could also be significantly increased by using (aminopropyl)triethoxysilane to covalently link ammonium ions to the surface.

Mesoporous nanospace can supply an environment where molecular motions and orientations are highly limited. This situation is similar to that in the confined spaces found in enzyme pockets, so that mesoporous nanospace should be a good medium for performance of biomimetic functions. Pirngruber and coworkers immobilized histidine and glutamic acid residues on the surface of mesoporous silica supports to construct an Fe(II) complex as a biomimetic catalyst (Fig. 20A) [198]. The biomimetic iron complexes obtained were tested as catalysts for cyclohexane oxidation under mild reaction conditions with hydrogen peroxide as oxidant. The nature of the immobilized amino acid and its surface density has an influence on the catalytic activity. Lin and coworkers dispersed copper complexes in mesoporous silica to study the abilities of model systems in the catalytic oxidation of *o*-diphenol to *o*-quinone by employing 3,5-di-*tert*-butylcatechol to test the catecholase activity of dicupric complexes [199]. The corresponding reaction cycle is depicted in Fig. 20. Initially, the acidic protons are abstracted from 3,5-di-*tert*-butylcatechol by addition of base. The negatively charged 3,5-di-*tert*-butylcatechol will coordinate to the *met* form of dinuclear Cu(II) complex and form the dicopper–catechol complex (*met*-D) as an intermediate. 3,5-Di-*tert*-butylquinone is formed in a two-electron redox reaction. The Cu(II) ions are reduced to the deoxy state of Cu(I) ions by removal of the hydroxo bridge during the uptake of a proton and release of a water molecule. Then dioxygen can bind to the dinuclear Cu(I) complex, forming an oxy state of the dinuclear Cu(II) complex. The function of dioxygen in the catalytic reaction is a thermodynamic driving process, in which any nascent Cu(I) species are reoxidized back to the active Cu(II) species and begin another catalytic cycle.

In biological systems, functional molecules such as chromophores and vitamins play unique roles within well-defined structures. Therefore, confining such functional molecules into mesopore nanospaces introduces attractive research possibilities. Durrant and coworkers reported the spectroelectrochemical investigation of proton-coupled electron transfer in flavodoxin D. vulgaris Hildenborough immobilized on nanocrystalline mesoporous SnO_2 electrodes with the aid of poly-L-lysine [200]. Such electrodes are suitable for addressing relatively slow redox events and, in this case, they applied the electrode to a study of the kinetics of deprotonation associated with the oxidation of flavodoxin semiquinone to its quinone state. Itoh et al. prepared a chlorophyll-mesoporous silica (FSM) conjugate with high photo-stability [201]. The mesopore spaces of the FSM also allow nanoscale interactions between the absorbed chlorophyll molecules. The conjugate can evolve hydrogen gas efficiently in the presence of an electron donor, a carrier, and a catalyst and upon visible light illumination. In another report, they investigated the arrangement of chlorophyll molecules within mesoporous nanospaces [202]. The arrangement of chlorophylls and the distance between the porphyrin rings are both important in determining the molecular interaction that leads to the changes in absorption/fluorescence behavior, energy transfer efficiency, and charge separation probability. Their spectroscopic experiments suggest that the arrangement of chlorophyll molecules inside each nanoscale pore of FSM-22 (pore diameter, 4.0 nm) resembles that in light-harvesting or reaction-center complexes of living plants (Fig. 21(a)). That is, they exhibit red-shifted spectral forms and fast energy transfer. In contrast, FSM-10 with a smaller pore (pore diameter, 1.9 nm) is expected to have chlorophyll aggregates inside or outside the FSM (Fig. 21(b) and (c)), which seem to exist too far apart to allow efficient energy transfer. These examples illustrate the importance of selection of appropriate mesoporous nanospace for promoted functions. Meyer and coworkers immobilized hemin (chloro(protoporhyrinato)iron(III)) at mesoporous nanocrystalline (anatase) TiO_2 thin films [203]. Reactions of heme/TiO_2(e^-) with CCl_4 or 1,1-bis(*p*-chlorophenyl)-2,2,2-trichloroethane led to the formation of stable carbene products in greater than 60% yield. The spectroscopic data provided compelling evidence for production of carbene, and constituted direct proof of a two-electron-transfer pathway (Fig. 22A). The organohalide may coordinate to the heme prior to electron transfer in an inner-sphere-type mechanism or the: CR_2 products may be trapped by the Fe(II) center after outer-sphere electron transfer. Asaftei and Walder cross-linked the vitamin B_{12} derivatives equipped with multiple reaction sites in the TiO_2 mesopores (Fig. 22B) [204]. The cross-linkers have multiple functions with one of them assisting the electron transfer from TiO_2 to the Co centers through redox shuttling. The modified electrodes show high electrocatalytic reactivity toward organic halides as well as improved stability.

Several investigations of amphiphilic peptide derivatives have demonstrated their capabilities as shape-defined molecular assemblies. These peptide amphiphiles can be used for mesostructuring of silica-peptide conjugates. Naik and coworkers reported synthesis of mesoporous silica with poly(L-lysine) as structure-directing reagent and demonstrated the polypeptide secondary structure transition that occurs during the silicification reaction [205]. Formation of the hexagonal silica platelets is attributed to the peptide helical chains that are formed in the presence of monosilicic acid and phosphate ions. The molecular weight of polypeptide was also found to affect the morphology of the resulting silica precipitate. Higher molecular weights of the peptide produced hexagonal silica platelets, whereas spherical silica particles were obtained using low-molecular weight peptide. The mesoporous materials confining the peptide segments in highly organized mesopore nanospace were developed by Ariga et al. (Fig. 23A) using peptide amphiphiles [206–208], which bear a polar quaternary ammonium salt at the pep-

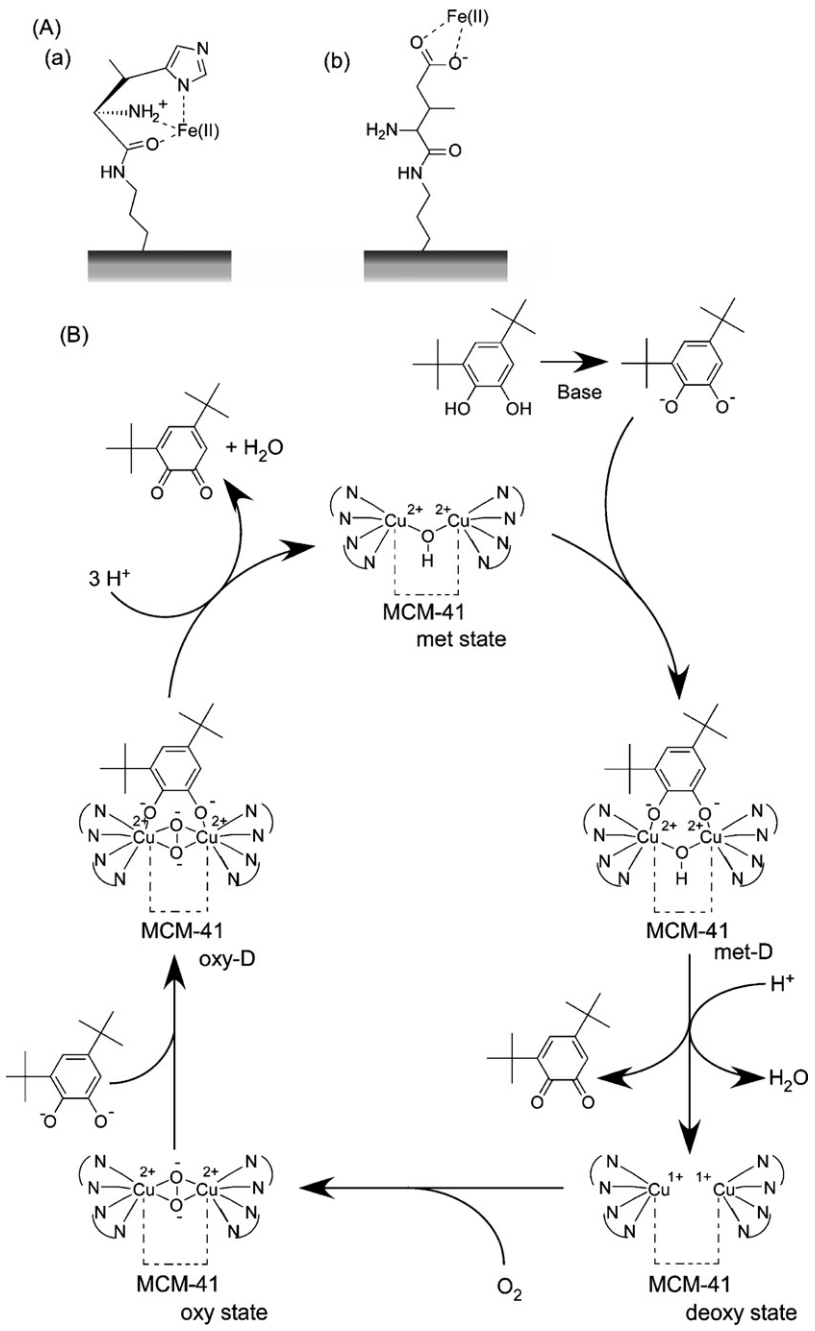

Fig. 20. (A) Fe complex as biomimetic catalyst. (B) Catecholase activity by dicupric complex. Reprinted with permission from [199], ©2005, American Chemical Society.

tide N-terminal and hydrophobic alkyl chain at the C-terminal were used as template for mesoporous silica in both transparent film and powder form. TEM images of the films indicate highly ordered regular pore arrays (Fig. 23B). Photochromic dye molecules such as spiropyran can be doped in the chiral environments of the silica-peptide conjugate films, where asymmetric photoreaction was demonstrated (Fig. 23C). Alanylalanine-type amphiphiles, named LL and DD denoting the chirality of the peptide moiety, were used as the host peptides in transparent mesoporous silica films, where spiropyran guest was co-doped with the peptides. Isomerization between spiropyran and merocyanine forms can be repeated upon alternate irradiation of the films by visible light (420 nm) and UV light (280 nm), respectively. Negligible circular dichroism (CD) signals originating from the guest were observed for the film containing the merocyanine form, but the film with the spiropyran form showed clear CD activity. Alternate irradiation with UV and visible light induced repeated changes in the CD spectra with a small degradation in the intensity. In addition, a complete mirror image of the CD spectra was obtained when the DD was used as the host surfactant. The presented materials are expected to be applied to memory devices with non-destructive read-out capability.

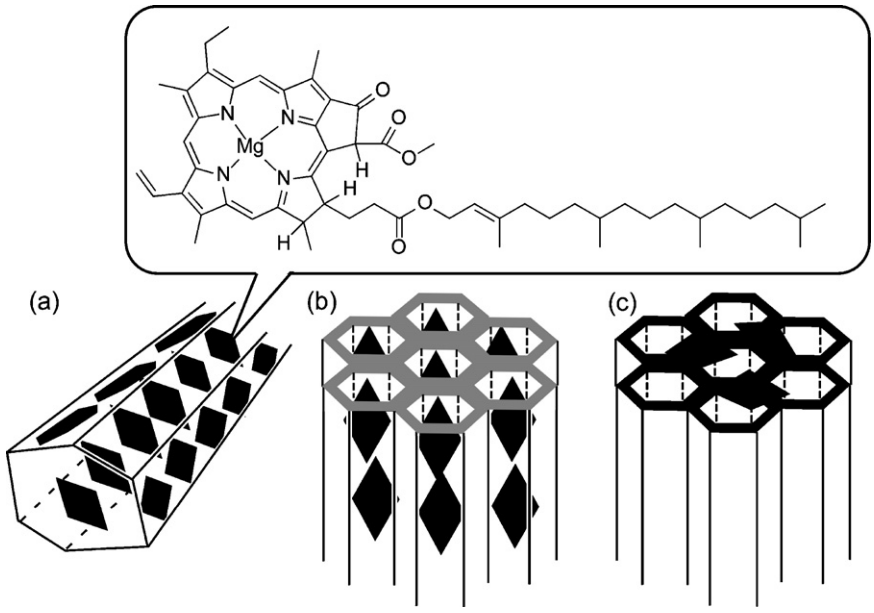

Fig. 21. Chlorophyll arrangement in mesopores: (a) FMS-22; (b) and (c) FMS-10. Reprinted with permission from [202], ©2004, American Chemical Society.

2.6. Photo-electronic functions

In the previous section several examples illustrate the attractiveness of photo-electronic functions as targets in research on mesoporous materials. Photo-electronically functional molecules can form specific arrangements in mesopore nanospaces, possibly leading to novel functions that cannot be attained in open spaces.

Molecular arrangements on solid substrates play an important role in vital functions such as photosynthesis and preparation of artificially ordered molecular structures is attractive from the life scientific or optoengineering points of view. Wada and coworkers reported reversible transformation between monomers and J-aggregates of 5,10,15,20-tetraphenyl-21H,23H-porphine-*p*,*p*′,*p*′,*p*‴-tetrasulfonic acid tetrasodium salt hydrate in mesoporous TiO_2 films [209]. The assembling behaviors of the dye molecules doped within mesopore nanospace depend on the pH value, which was not previously observed in solution open space. García and coworkers synthesized a series of periodic mesoporous silicates of MCM-41 type containing chiral binaphthyl and cyclohexadiyl moieties occupying framework positions [210]. Chiral discrimination was also demonstrated by measuring the photoluminescence of the chiral organosilicas in the presence of enantiomerically pure quenchers. Ozin and coworkers reported the electrochromic performance of viologen-modified periodic mesoporous nanocrystalline anatase [211]. The well-ordered mesostructured, nanocrystalline TiO_2 electrode exhibit similar color switching speed and reversibility as nanocrystalline titania but with better performance in terms of color contrast. This performance can be attributed to a contiguous pathway of well-connected anatase nanocrystallites arranged into a well-defined mesoporous architecture, which results in a greater volume density of tethered chromophore molecules. Carlos and coworkers synthesized the mesoporous silica MCM-41 functionalized with a chelating pyrazolylpyridine ligand as a support for the immobilization of coordination complexes of Eu(III) and Gd(III) (Fig. 24) [212]. Spectroscopic studies, supported by ab initio calculations, provided strong evidence that the immobilized Eu(III) complex is 8-coordinate. The tethering procedure leads to isolation of complexes from the siliceous support, thus minimizing any possible interactions with residual surface silanols that could lead to luminescence quenching. Design of new luminescent displays should now be possible using highly oriented MCM-41 films impregnated with emitting centers showing enhanced antenna effects. Fu and coworkers successfully incorporated the luminescent lanthanide complex, $Eu(phen)_2Cl_3$ (phen = 1,10-phenanthroline) inside the channels of mesoporous silica MCM-41 with its external surface modified by phenyltriethoxysilane via a simple template-ion exchange method [213]. The resulting hybrid material exhibited the characteristic emission of Eu(III) ions under UV irradiation with higher luminescence quantum efficiency, longer lifetime and better thermal stability than the corresponding pure complex. The characterization results show that the local symmetry and first coordination shell of Eu(III) ions change after the complex ions are incorporated into the MCM-41 channels and that a more symmetric environment is occupied by the Eu ions in mesoporous hybrids than in the pure complex. A more efficient ligand-to-Eu(III) intramolecular energy transfer process was observed in the conjugate with mesoporous silica. Aida and coworkers reported the first example of immobilization of one-dimensional columnar charge-transfer assemblies in a mesoporous silica film through sol-gel reaction with charge-transfer complexes of amphiphilic triphenylene donor and various acceptors (Fig. 25) [214]. The films obtained are highly transparent and color-tunable by variation of the intercalating acceptor. The silica wall segregates the individual charge-transfer columns, which display neither solvatochromism nor guest exchange activity and exhibit red-shifted absorption bands, which are possibly due to a long-range

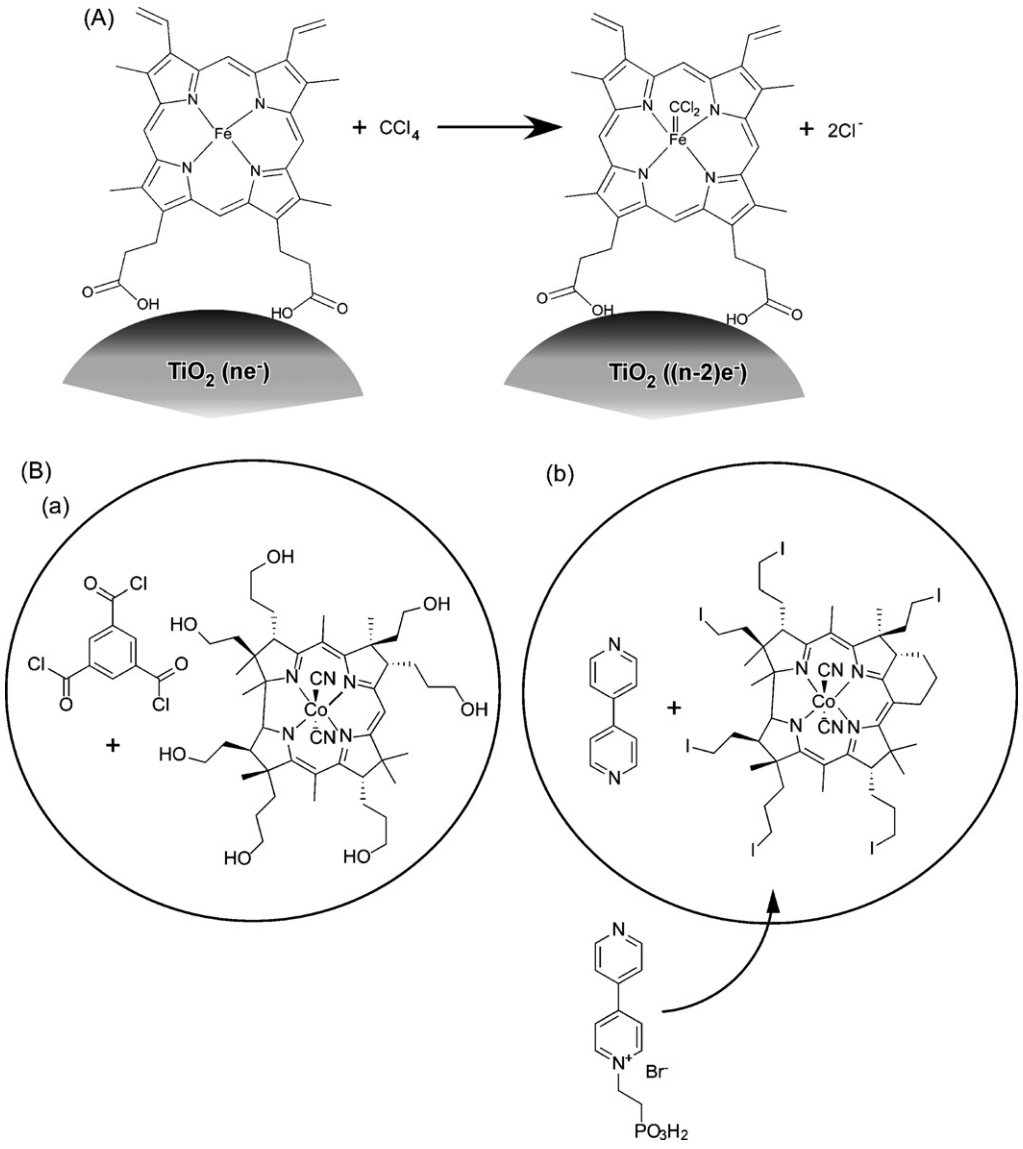

Fig. 22. (A) Biomimetic catalysis by hemin immobilized mesoporous TiO_2. (B) TiO_2 mesopore modified with cross-linked vitamin B_{12} function. Reprinted with permission from [203,204], ©2006, American Chemical Society.

structural ordering. The donor/acceptor molar ratio, related to photoconductive properties, can be varied over a wide range from 1:1 to 9:1.

Conjugate polymers are powerful candidates as functional modules for photo-electron function. Therefore, preparation of mesoporous materials possessing conjugated polymers in their mesopores is an attractive research target. Peculiar physico-chemical properties could result because the length of conjugated polymers exceeds the dimension of pore diameter, and motion and orientation of the confined polymers would be highly restricted. Schwartz and coworkers reported incorporation of poly[phenylene vinylene] derivatives and energy migration along the incorporated polymer [215]. Ozin and coworkers demonstrated ring-opening polymerization of [1]silaferrocenophane in MCM-41 to provide poly(ferrocenylsilanes) [216]. Pyrolysis of the composite at 1173 K resulted in formation of iron oxide nanoparticles exhibiting superparamagnetism. Choi and coworkers prepared polyaniline–silica nanocomposites by polymerization of aniline gas in MCM-41 mesopores [217]. Jang et al. proposed formation of coaxial nanocables prepared inside the pore channels of SBA-15 mesoporous silica through sequential polymerization of methyl methacrylate and pyrrole [218]. Aida and Tajima used a few kinds of hexadecadiynyl trimethylammonium bromide as templates to synthesize mesoporous silica containing diacetylene as a micro-fiber [219]. Confinement effects of the polydiacetylene appeared as an elongated effective conjugation in the silica nanochannel. The same research group developed poly(pyrrole)-containing mesoporous silica film [220]. The polypyrrole chains are highly constrained and insulated when incorporated within hexagonal nanoscopic channels and the possibility of polarons recombining into bipolarons is significantly suppressed. In contrast, a two-dimensional lamellar phase afforded spatial freedom for the electron recombination. Thiophene polymerization in mesoporous silica channel was reported by Fuhrhop and coworkers [221]. Lu et al. used oligo(ethylene glycol)-functionalized

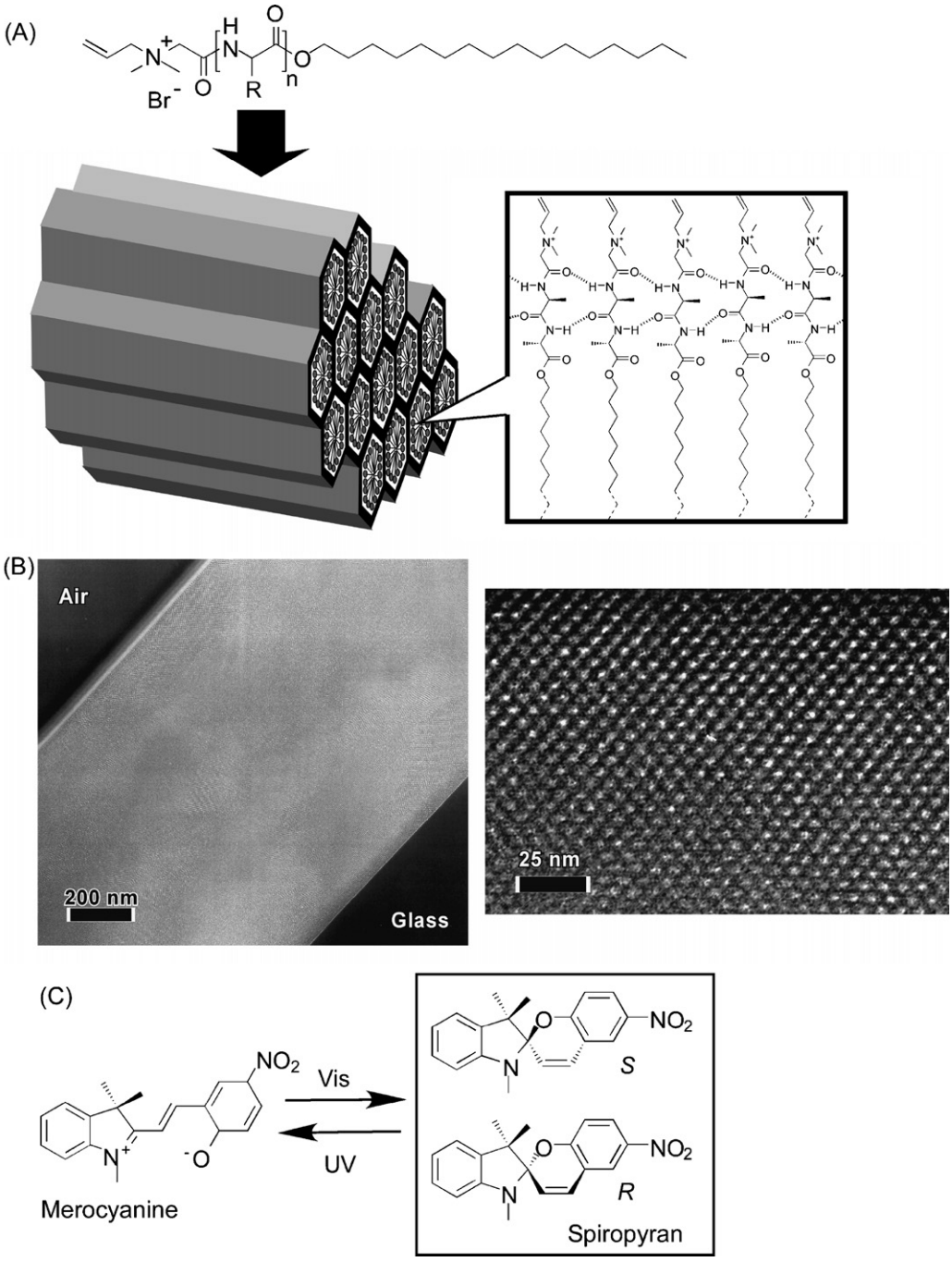

Fig. 23. Peptide-immobilized mesoporous silica and its function: (A) schematic illustration of structure; (B) TEM images: (C) asymmetric reaction conducted in mesopore.

diacetylenic surfactants as structure-directing reagents for mesoporous silica film [222]. The resulting nanocomposites displayed unusual chromatic changes in response to thermal, mechanical, and chemical stimuli. Lin et al. reported the synthesis of Cu^{2+}-functionalized MCM-41 silica and alumina, which can oxidatively catalyze the formation of a highly conjugated poly(phenylene butadiynylene) polymer (Fig. 26A) [223]. Fluorescence and solid-state NMR provided spectroscopic evidence that the synthesis of extended polymeric chains with a high degree of alignment requires homogeneously distributed catalytic sites throughout the matrix. Robin and coworkers synthesized optically active nanostructured composite materials using an amphiphilic semiconducting polymer, 4-octyloxy-l-(2-trimethylammoniumethoxy)-2,5-poly(phenylene ethynylene) chloride (Fig. 26B) [224]. The polymer retains its photophysical properties in the composite, showing luminescence similar to polymers in the solution phase. The polymer displays a high degree of luminescence polarization anisotropy, indicating that the polymer chains are straight and mutually isolated in the composite. Lu and coworkers synthesized responsive PMO using silsesquioxanes containing a bridged diacetylenic group [225]. Topo-polymerization creates

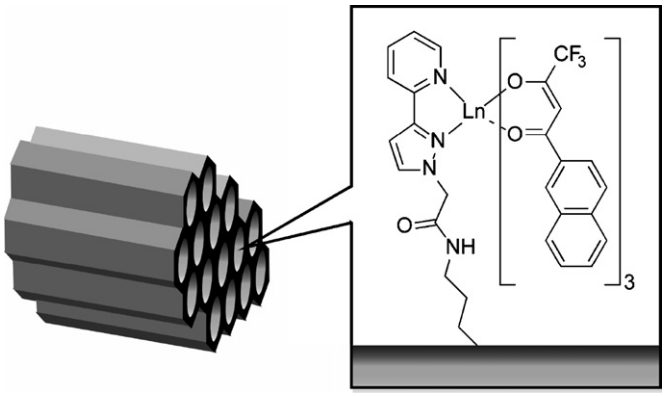

Fig. 24. Coordination complex of Ln (Eu and Gd) on mesoporous silica surface.

the responsive PMO embedded with polydiacetylene (PDA), a polymer that chromatically responds (e.g., blue to red) to a wide range of external stimuli (Fig. 26C). Garcia and coworkers also demonstrated a photoresponsive PMO that exhibited reversible change in adsorption capacity derived from the changes in the molecular dimensions of azobenzene in the trans and cis configuration [226]. Stupp and coworkers fabricated hybrid materials containing silicate and charged oligo(*p*-phenylene vinylene) amphiphiles by spin casting using evaporation-induced self assembly [227]. Extremely efficient energy transfer occurred in these materials from the electronically active polymer segments to rhodamine B dyes grafted covalently to the inorganic silicate domains of the periodic structure. Their results indicate that the ordered and nanostructured environment leads to highly efficient energy transfer among organic components in these hybrid films. As uniquely conjugated molecule, a fullerene C_{60} molecule was incorporated in mesoporous MCM-41 aluminosilicate and their second harmonic generation (SHG) enhancement was investigated by Bourdelande and coworkers [228]. In that case, SHG clearly depends on the nature of the host as well as on the nature of the alkali metal ion accompanying C_{60}, and an unprecedented two orders of magnitude enhancement of the SHG efficiency was observed. Apart from these examples, photo-electron properties using conjugated polymers confined with in mesopore nanospaces have been reported by others [219,229–231], as well as related research on mesoporous hybrids with low-molecular-weight functional molecules [232–235].

3. Future perspectives

In this review, various examples of coordination chemistry, supramolecular chemistry, and their related functions designed in mesoporous nanospaces have been introduced. Because mesopore size regulates orientation and arrangement of attached functional units ensuring free diffusion of interactive molecules, mesoporous nanospaces provide attractive environments for coordination and supramolecular chemistry. The ease of design of the mesoporous nanospaces makes them suitable for fundamental research in various fields, since well-defined size and mutual geometries of functional materials are available. Additionally, mesoporous materials introduce con-

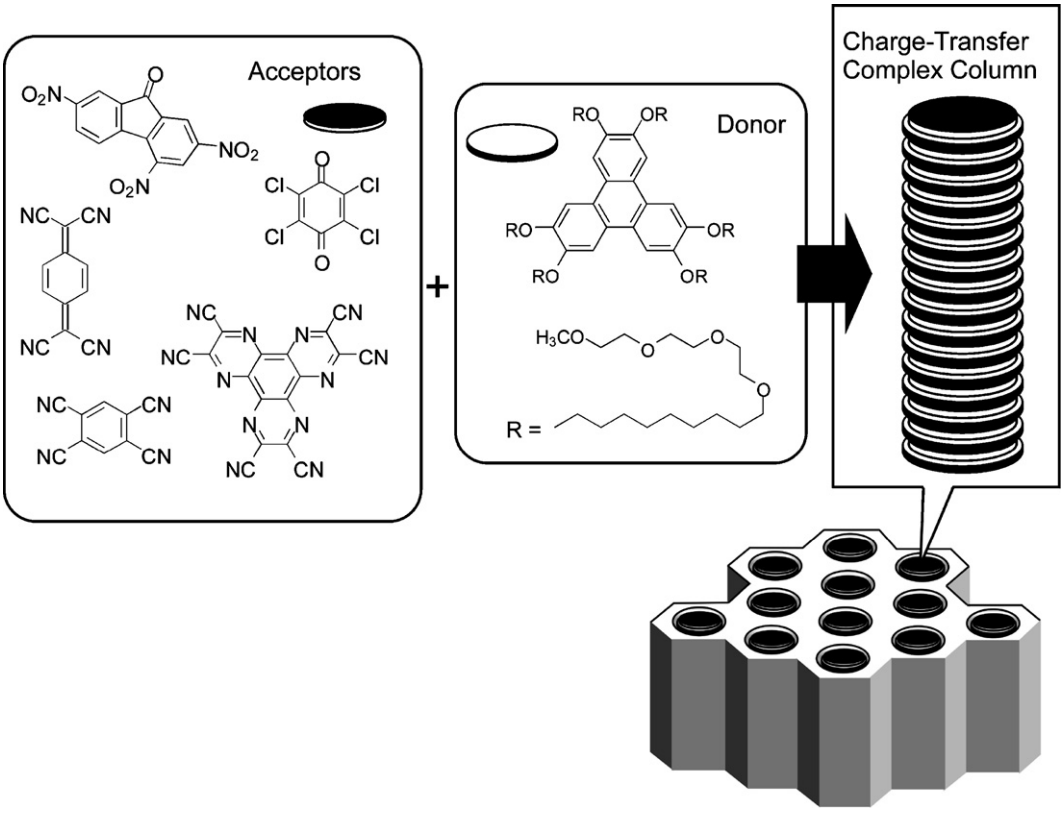

Fig. 25. Charge-transfer column confined in mesopore channel.

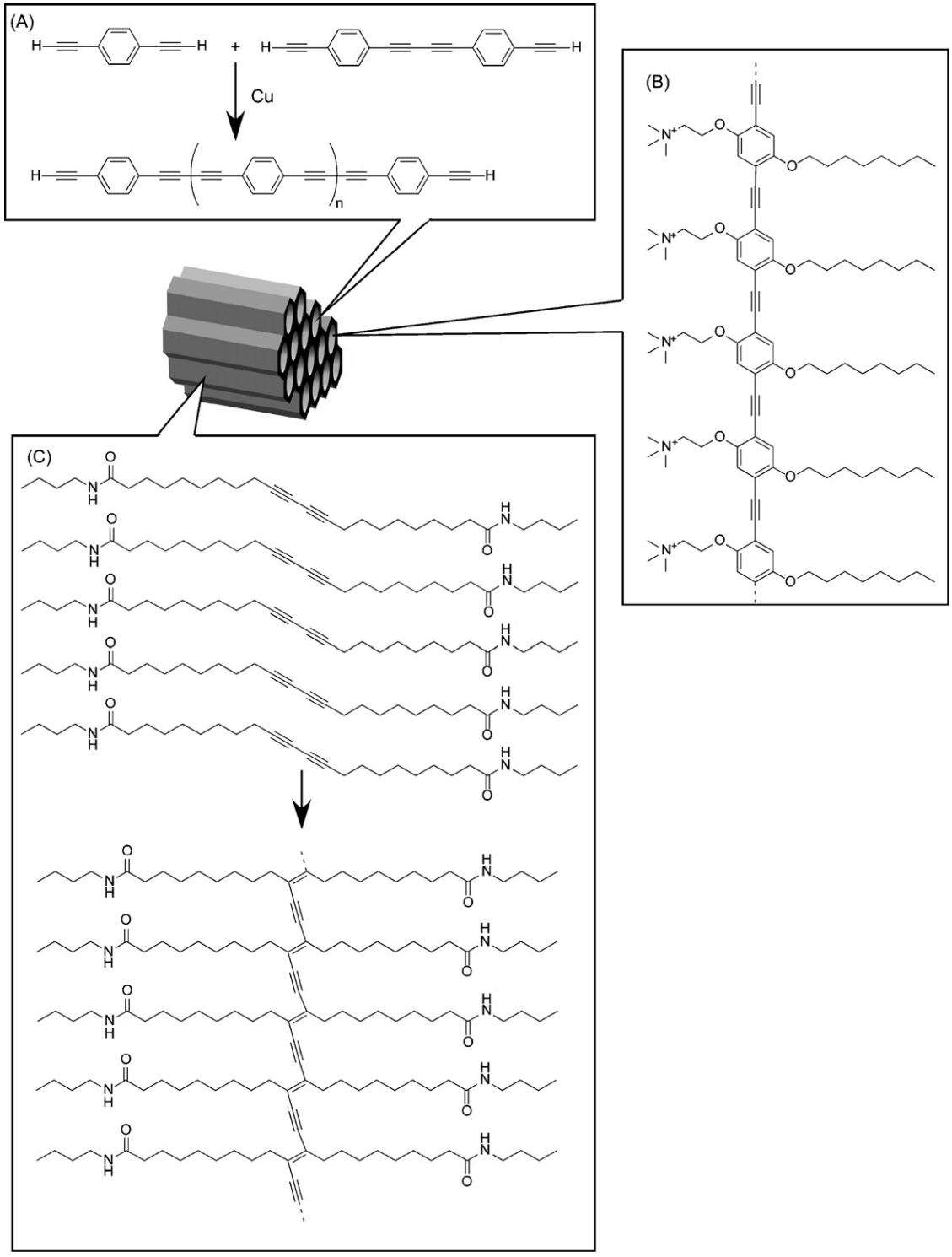

Fig. 26. Conjugate polymers confined within mesopores: (A) poly(phenylene butadiynylene); (B) poly(phenylene ethynylene); (C) poly(diacethylene).

siderable possibilities in application-oriented areas. Although we have selected examples from research published in the last few years, potential applications for the mesoporous silicates are diverse spanning the physical chemical and bio-medical realms. Mesoporous materials can be obtained in large volume from inexpensive materials according to well-established procedures, at the same time providing the aforementioned precisely dimension-controlled nanospaces. Therefore, mesopore nanospace is attractive for development of practical applications using advanced coordination and supramolecular chemistry techniques.

Mesoporous silica materials have been so far used in various fields because of well-established procedures in their synthesis and modification. However, silica itself does not usually pos-

sess advanced functionality. Several examples contained here indicate that mesoporous titania is applicable in practical applications. For example, Kavan and coworkers proposed design of dye-sensitized solar cells using a dye-included mesoporous TiO_2 film [236]. Mesoporous carbon would be another attractive candidate for many applications because it could show excellent electronic properties as seen in the other nanocarbons. Zhao and coworkers proposed use of mesoporous carbon CMK-3 for lithium-ion batteries [237]. Yu and coworkers demonstrated use of bimodal mesoporous carbon for a direct methanol fuel cell [238]. In addition and in contrast to silica, mesoporous carbon is totally hydrophobic. This environment should be useful to remove environmentally toxic bio-organic substances many of which are hydrophobic. Furthermore, a hydrophobic non-polar environment (or water-avoided environment) is advantageous for some kinds of molecular interaction including hydrogen bonding, electrostatic interactions, and coordination chemistry. Therefore, there are plenty of areas in which novel supramolecular and coordination chemistries can develop, and they exist in mesoporous nanospaces such as those composed of carbon.

Acknowledgement

This work was partly supported by Grant-in Aid for Scientific Research on Priority Areas (No. 18033059 “Chemistry of Coordination Space”) from Ministry of Education, Science, Sports, and Culture, Japan.

References

[1] A. Sayari, Chem. Mater. 8 (1996) 1840.
[2] A. Corma, Chem. Rev. 97 (1997) 2373.
[3] J.Y. Ying, C.P. Mehnert, M.S. Wong, Angew. Chem. Int. Ed. 38 (1999) 56.
[4] A. Hagfeldt, M. Gratzel, Acc. Chem. Res. 33 (2000) 269.
[5] Y. Tao, H. Kanoh, L. Abrams, K. Kaneko, Chem. Rev. 106 (2006) 896.
[6] J.A. Melero, R. van Grieken, G. Morales, Chem. Rev. 106 (2006) 3790.
[7] M. Vallet-Regí, Chem. Eur. J. 12 (2006) 5934.
[8] K. Moller, T. Bein, Chem. Mater. 10 (1998) 2950.
[9] U. Ciesla, F. Schüth, Micropor. Mesopor. Mater. 27 (1999) 131.
[10] H. Gleiter, Acta Mater. 48 (2000) 1.
[11] A. Stein, B.J. Melde, R.C. Schroden, Adv. Mater. 12 (2000) 1403.
[12] A.B. Descalzo, R. Martínez-Máñez, F. Sancenón, K. Hoffmann, K. Rurack, Angew. Chem. Int. Ed. 45 (2006) 5924.
[13] N.K. Raman, M.T. Anderson, C.J. Brinker, Chem. Mater. 8 (1996) 1682.
[14] Y. Liu, T.J. Pinnavaia, J. Mater. Chem. 12 (2002) 3179.
[15] M.E. Davis, Nature 417 (2002) 813.
[16] K. Ariga, J. Nanosci. Nanotechnol. 4 (2004) 23.
[17] A. Okabe, T. Fukushima, K. Ariga, M. Niki, T. Aida, J. Am. Chem. Soc. 126 (2004) 9013.
[18] G.E. Fryxell, Inorg. Chem. Commun. 9 (2006) 1141.
[19] K. Ariga, A. Vinu, M. Miyahara, Curr. Nanosci. 2 (2006) 197.
[20] A. Vinu, M. Miyahara, K. Ariga, J. Nanosci. Nanotechnol. 6 (2006) 1510.
[21] T. Yanagisawa, T. Shimizu, K. Kuroda, C. Kato, Bull. Chem. Soc. Jpn. 63 (1990) 988.
[22] S. Inagaki, Y. Fukushima, K. Kuroda, J. Chem. Soc., Chem. Commun. (1993) 680.
[23] C.T. Kresge, M.E. Leonowicz, W.J. Roth, J.C. Vartuli, J.S. Beck, Nature 359 (1992) 710.
[24] J.S. Beck, J.C. Vartuli, W.J. Roth, M.E. Leonowicz, C.T. Kresge, K.D. Schmitt, C.T.W. Chu, D.H. Olson, E.W. Sheppard, S.B. McCullen, J.B. Higgins, J.L. Schlenker, J. Am. Chem. Soc. 114 (1992) 10834.
[25] J.C. Vartuli, K.D. Schmitt, C.T. Kresge, W.J. Roth, M.E. Leonowicz, S.B. McCullen, S.D. Hellring, J.S. Beck, J.L. Schlenker, D.H. Olson, E.W. Sheppard, Chem. Mater. 6 (1994) 2317.
[26] M. Dubois, T. Gulik-Krzywicki, B. Cabane, Langmuir (1993) 673.
[27] P.T. Tanev, T.J. Pinnavaia, Science 267 (1995) 865.
[28] S.A. Bagshaw, E. Prouset, T.J. Pinnavaia, Science 269 (1995) 1242.
[29] D. Zhao, J. Feng, Q. Huo, N. Melosh, G.H. Fredickson, B.F. Chmelka, G.D. Stucky, Science 279 (1998) 548.
[30] D. Zhao, Q. Huo, J. Feng, B.F. Chmelka, G.D. Stucky, J. Am. Chem. Soc. 120 (1998) 6024.
[31] P. Schmidt-Winkel, W.W. Lukens, D. Zhao, P. Yang, B.F. Chmelka, G.D. Stucky, J. Am. Chem. Soc. 121 (1999) 254.
[32] Y. Yue, Y. Sun, Z. Gao, Catal. Lett. 47 (1997) 167.
[33] B.P. Kelleher, A.M. Doyle, T.F. O’Dwyer, B.K. Hodnett, J. Chem. Technol. Biotechnol. 76 (2001) 1216.
[34] S. Che, A.E. Garcia-Benett, T. Tokoi, K. Sakamoto, H. Kunieda, O. Terasaki, T. Tatsumi, Nat. Mater. 2 (2003) 801.
[35] Y.C. Liang, M. Hanzlik, R. Anwander, Chem. Commun. (2005) 525.
[36] D.M. Antonelli, J.Y. Ying, Angew. Chem. Int. Ed. Engl. 34 (1995) 2014.
[37] R. Takahashi, S. Takenaka, S. Sato, T. Sodesawa, K. Ogura, K. Nakanishi, J. Chem. Soc., Faraday Trans. 94 (1998) 3161.
[38] U. Bach, D. Lupo, P. Comte, J.E. Moser, F. Weissörtle, J. Salbeck, H. Spreitzer, M. Gratzel, Nature 395 (1998) 583.
[39] P. Yang, D. Zhao, D.I. Margolese, B.F. Chmelka, G.D. Stucky, Chem. Mater. 11 (1999) 2813.
[40] D. Grosso, G.J.deA.A. Soler-Illia, F. Babonneau, C. Sanchez, P.-A. Albouy, A. Brunet-Bruneau, A.R. Balkenende, Adv. Mater. 13 (2001) 1085.
[41] P.C.A. Alberius, K.L. Frindell, R.C. Hayward, E.J. Kramer, G.D. Stucky, B.F. Chmelka, Chem. Mater. 14 (2002) 3284.
[42] F.-S. Xiao, Y. Han, Y. Yu, X. Meng, M. Yang, S. Wu, J. Am. Chem. Soc. 124 (2002) 888.
[43] M. Vettraino, M. Trudeau, A.Y.H. Lo, R.W. Schurko, D. Antonelli, J. Am. Chem. Soc. 124 (2002) 9567.
[44] R.C. Hayward, B.F. Chmelka, E.J. Kramer, Adv. Mater. 17 (2005) 2591.
[45] T. Streethawong, Y. Suzuki, S. Yoshikawa, J. Solid State Chem. 178 (2005) 329.
[46] D.M. Antonelli, J.Y. Ying, Chem. Mater. 8 (1996) 874.
[47] H. Kosslick, G. Lischke, G. Walther, W. Storek, A. Martin, R. Fricke, Microporous Mater. 9 (1997) 13.
[48] J.N. Kondo, L. Lu, Y. Takahara, K. Maruya, K. Domen, N. Igarashi, T. Tatsumi, Bull. Chem. Soc. Jpn. 73 (2000) 1123.
[49] D. Antonelli, J.Y. Ying, Angew. Chem. Int. Ed. Engl. 35 (1996) 426.
[50] D.M. Antonelli, A. Nakahira, J.Y. Ying, Inorg. Chem. 35 (1996) 3126.
[51] F. Schüth, U. Ciesla, S. Schacht, M. Thieme, Q. Huo, G.D. Stucky, Mater. Res. Bull. 34 (1999) 483.
[52] B.T. Holland, C.F. Blanford, T. Do, A. Stein, Chem. Mater. 11 (1999) 795.
[53] M.S. Wong, J.Y. Ying, Chem. Mater. 10 (1998) 2067.
[54] S.A. Bagshaw, E. Prouzet, T.J. Pinnavaia, Science 269 (1995) 1242.
[55] S.A. Bagshaw, T.J. Pinnavaia, Angew. Chem. Int. Ed. Engl. 35 (1996) 1102.
[56] F. Vaudry, S. Khodabandeh, M.E. Davis, Chem. Mater. 8 (1996) 1451.
[57] P. Liu, I.L. Moudrakovski, J. Liu, A. Sayari, Chem. Mater. 9 (1997) 2513.
[58] J. Lee, S. Yoon, T. Hyeon, S.M. Oh, K.B. Kim, Chem. Commun. (1999) 2177.
[59] J. Lee, S. Yoon, S.M. Oh, C.-H. Shin, T. Hyeon, Adv. Mater. 12 (2000) 359.
[60] F. Schüth, Chem. Mater. 13 (2001) 3184.
[61] R. Ryoo, S.H. Joo, M. Kruk, M. Jaroniec, Adv. Mater. 13 (2001) 677.
[62] S.H. Joo, S.J. Choi, I. Oh, J. Kwak, Z. Liu, O. Terasaki, R. Ryoo, Nature 412 (2001) 169.
[63] L.A. Solovyov, V.I. Zaikovskii, A.N. Shmakov, O.V. Belousov, R. Ryoo, J. Phys. Chem. B 106 (2002) 12198.
[64] S. Han, S. Kim, H. Lim, W. Choi, H. Park, J. Yoon, T. Hyeon, Micropor. Mesopor. Mater. 58 (2003) 131.
[65] T. Kyotani, Bull. Chem. Soc. Jpn. 79 (2006) 1322.
[66] R. Ryoo, S.H. Joo, S. Jun, J. Phys. Chem. B 103 (1999) 7743.

[67] S. Jun, S.H. Joo, R. Ryoo, M. Kurk, M. Jaroniec, Z. Liu, T. Ohsuna, O. Terasaki, J. Am. Chem. Soc. 122 (2000) 10712.
[68] A. Vinu, M. Miyahara, K. Ariga, Stud. Surf. Sci. Catal. 158 (2005) 971.
[69] A. Vinu, M. Miyahara, V. Sivamurugan, T. Mori, K. Ariga, J. Mater. Chem. 15 (2005) 5122.
[70] A. Vinu, M. Miyahara, T. Mori, K. Ariga, J. Porous Mater. 13 (2006) 379.
[71] A. Vinu, K. Ariga, T. Mori, T. Nakanishi, S. Hishita, D. Golberg, Y. Bando, Adv. Mater. 17 (2005) 1648.
[72] A. Vinu, M. Terrones, D. Golberg, S. Hishita, K. Ariga, T. Mori, Chem. Mater. 17 (2005) 5887.
[73] S. Inagaki, S. Guan, Y. Fukushima, T. Ohsuna, O. Terasaki, J. Am. Chem. Soc. 121 (1999) 9611.
[74] S. Inagaki, S. Guan, T. Ohsuna, O. Terasaki, Nature 416 (2002) 304.
[75] M.P. Kappor, S. Inagaki, Bull. Chem. Chem. Jpn. 79 (2006) 1463.
[76] T. Asefa, M.J. MacLachlan, N. Coombs, G.A. Ozin, Nature 402 (1999) 867.
[77] B.J. Melde, B.T. Holland, C.F. Blanford, A. Stein, Chem. Mater. 11 (1999) 3302.
[78] A. Vinu, K.Z. Hossain, K. Ariga, J. Nanosci. Nanotechnol. 5 (2005) 347.
[79] T. Maschmeyer, F. Rey, G. Sankar, J.M. Thomas, Nature 378 (1995) 159.
[80] M.H. Lim, A. Stein, Chem. Mater. 11 (1999) 3285.
[81] A. Walcarius, M. Etienne, B. Lebeau, Chem. Mater. 15 (2004) 2161.
[82] S.L. Burkett, S.D. Sims, S. Mann, Chem. Commun. (1996) 1367.
[83] L. Mercier, T.J. Pinnavaia, Chem. Mater. 12 (2000) 188.
[84] Z. Yan, G. Li, L. Mu, S. Tao, J. Mater. Chem. 16 (2006) 1717.
[85] Z. Yan, S. Tao, J. Yin, G. Li, J. Mater. Chem. 16 (2006) 2347.
[86] D. Pérez-Quintanilla, I. del Hierro, M. Fajardo, I. Sierra, J. Mater. Chem. 16 (2006) 1757.
[87] K.H. Nam, L.L. Tavlarides, Chem. Mater. 17 (2005) 1597.
[88] X. Xu, Y. Han, D. Li, H. Ding, Y. Wang, F.-S. Xiao, Chem. Mater. 16 (2004) 3507.
[89] S.J.L. Billinge, E.J. McKimmy, M. Shatnawi, H.J. Kim, V. Petkov, D. Wermeille, T.J. Pinnavaia, J. Am. Chem. Soc. 127 (2005) 8492.
[90] K.F. Lam, K.L. Yeung, G. McKay, Langmuir 22 (2006) 9632.
[91] M. Benitez, D. Das, R. Ferreira, U. Pischel, H. García, Chem. Mater. 18 (2006) 5597.
[92] O. Olkhovyk, S. Pikus, M. Jaroniec, J. Mater. Chem. 15 (2005) 1517.
[93] J. Alauzun, A. Mehdi, C. Reyé, R.J.P. Corriu, J. Am. Chem. Soc. 128 (2006) 8718.
[94] M. Jaroniec, Nature 442 (2006) 638.
[95] G. Rodríguez-Lópwz, M.D. Marcos, R. Martínez-Máñez, F. Sancenón, J. Soto, L.A. Villaescusa, D. Beltrán, P. Amorós, Chem. Commun. (2004) 2198.
[96] H. Yoshitake, T. Yokoi, T. Tatsumi, Chem. Mater. 15 (2003) 1713.
[97] C. Liu, J.B. Lambert, L. Fu, J. Mater. Chem. 14 (2004) 1303.
[98] R.J.P. Corriu, A. Mehdi, C. Reyé, C. Thieuleux, New J. Chem. 27 (2003) 905.
[99] R.J.P. Corriu, A. Mehdi, C. Reyé, C. Thieuleux, A. Frenkel, A. Gilbaud, New. J. Chem. 28 (2004) 156.
[100] R.J.P. Corriu, E. Lancelle-Beltran, A. Mehdi, C. Reyé, S. Brandès, R. Guilard, J. Mater. Chem. 12 (2002) 1355.
[101] H. Wang, F.L.Y. Lam, X. Hu, K.M. Ng, Langmuir 22 (2006) 4583.
[102] E. Nakamura, H. Isobe, Acc. Chem. Res. 36 (2003) 807.
[103] K. Inumaru, Y. Inoue, S. Kakii, T. Nakano, S. Yamanaka, Chem. Lett. 32 (2003) 1110.
[104] K. Inumaru, Y. Inoue, S. Kakii, T. Nakano, S. Yamanaka, Phys. Chem. Chem. Phys. 6 (2004) 3133.
[105] S. Kim, E. Marand, Chem. Mater. 18 (2006) 1149.
[106] B. Lei, B. Li, H. Zhang, S. Lu, Z. Zheng, W. Li, Y. Wang, Adv. Funct. Mater. 16 (2006) 1883.
[107] H. Zhang, Y. Sun, K. Ye, P. Zhang, Y. Wang, J. Mater. Chem. 15 (2005) 3181.
[108] E. Coronado, J.R. Galán-Mascarós, C. Martí-Gastaldo, E. Palomares, J.R. Durrant, R. Vilar, M. Gratzel, M.K. Nazeeruddin, J. Am. Chem. Soc. 127 (2005) 12351.
[109] M.K. Nazeeruddin, D.D. Censo, R. Humphry-Baker, M. Gräzel, Adv. Funct. Mater. 16 (2006) 189.
[110] R. Métivier, I. Leray, B. Lebeau, B. Valeur, J. Mater. Chem. 15 (2005) 2965.
[111] H. Zhang, P. Zhang, K. Ye, Y. Sun, S. Jiang, Y. Wang, W. Pang, J. Lumin. 117 (2006) 68.
[112] B. García-Acosta, M. Comes, J.L. Bricks, M.A. Kudinova, V.V. Kurdyukov, A.I. Tolmachev, A.B. Descalzo, M.D. Marcos, R. Martínez-Máñez, A. Moreno, F. Sancenón, J. Soto, L.A. Villaescusa, K. Rurack, J.M. Barat, I. Escriche, P. Amorós, Chem. Commun. (2006) 2239.
[113] M. Comes, M.D. Marcos, R. Martínez-Máñez, M.C. Millán, J.V. Ros-Lis, F. Sancenón, J. Soto, L.A. Villaescusa, Chem. Eur. J. 12 (2006) 2162.
[114] A.B. Descaizo, K. Rurack, H. Weisshoff, R. Martínez-Máñez, M.D. Marcos, P. Amorós, K. Hoffman, J. Soto, J. Am. Chem. Soc. 127 (2005) 184.
[115] M. Comes, M.D. Marcos, R. Martínez-Máñez, F. Sancenón, J. Soto, L.A. Villaescusa, P. Amorós, D. Beltrán, Adv. Mater. 20 (2004) 1783.
[116] S. Basurto, T. Torroba, M. Comes, R. Martínez-Máñez, F. Sancenón, L. Villaescusa, P. Amorós, Org. Lett. 7 (2005) 5469.
[117] A.B. Descaizo, M.D. Marcos, R. Martínez-Máñez, J. Soto, D. Beltrán, P. Amorós, J. Mater. Chem. 15 (2005) 2721.
[118] M. Comes, G. Rodríguez-Lópwz, M.D. Marcos, R. Martínez-Máñez, F. Sancenón, J. Soto, L.A. Villaescusa, P. Amorós, D. Beltrán, Angew. Chem. Int. Ed. 44 (2005) 2918.
[119] S. Huh, H.-T. Chen, J.W. Wiench, M. Pruski, V.S.-Y. Lin, J. Am. Chem. Soc. 126 (2004) 1010.
[120] H.-T. Chen, S. Huh, J.W. Wiench, M. Pruski, V.S.-Y. Lin, J. Am. Chem. Soc. 127 (2005) 13305.
[121] T. Kageyama, T. Sakai, M. Matsuoka, M. Anpo, J. Am. Chem. Soc. 127 (2005) 16784.
[122] V. Dufaud, F. Beauchesne, L. Bonnevoit, Angew. Chem. Int. Ed. 44 (2005) 2.
[123] A.R. Silva, K. Wilson, A.C. Whitwood, J.H. Clark, C. Freire, Eur. J. Inorg. Chem. (2006) 1275.
[124] D. Khushalani, S. Hasenzahl, S. Mann, J. Nanosci. Nanotechnol. 1 (2001) 129.
[125] E.R. Leite, N.L.V. Carreno, E. Longo, A. Valentini, L.F.D. Probst, J. Nanosci. Nanotechnol. 2 (2002) 89.
[126] A. Vinu, K. Ariga, S. Saravanamurugan, M. Hartmann, V. Murugesan, Micropor. Mesopor. Mater. 76 (2004) 91.
[127] A. Vinu, M. Karthik, M. Miyahara, V. Murugesan, K. Ariga, J. Mol. Catal. A-Chem. 230 (2005) 151.
[128] A. Vinu, D.P. Sawant, K. Ariga, M. Hartmann, S.B. Halligudi, Micropor. Mesopor. Mater. 80 (2005) 195.
[129] A. Vinu, G.S. Kumar, K. Ariga, V. Murugesan, J. Mol. Catal. A-Chem. 235 (2005) 57.
[130] T. Krithiga, A. Vinu, K. Ariga, B. Arabindoo, M. Palanichamy, V. Murugesan, J. Mol. Catal. A-Chem. 237 (2005) 238.
[131] A. Vinu, D.P. Sawant, K. Ariga, K.Z. Hossain, S.B. Halligudi, M. Hartmann, M. Nomura, Chem. Mater. 17 (2005) 5339.
[132] A. Vinu, T. Krithiga, V.V. Balasubramanian, A. Asthana, P. Srinivasu, T. Mori, K. Ariga, G. Ramanath, P.G. Ganesan, J. Phys. Chem. B 110 (2006) 11924.
[133] A. Vinu, P. Srinivasu, M. Miyahara, K. Ariga, J. Phys. Chem. B 110 (2006) 801.
[134] R. Nakamura, H. Frei, J. Am. Chem. Soc. 128 (2006) 10668.
[135] C.M. Crudden, M. Sateesh, R. Lewis, J. Am. Chem. Soc. 127 (2005) 10045.
[136] C. Yue, M. Trudeau, D. Antonelli, Chem. Commun. (2006) 1918.
[137] Q. Yang, S. Ma, J. Li, F. Xiao, H. Xiong, Chem. Commun. (2006) 2495–2497.
[138] M. Andersson, H. Birkedal, N.R. Franklin, T. Ostomel, S. Boettcher, A.E.C. Palmqvist, G.D. Stucky, Chem. Mater. 17 (2005) 1409.
[139] F. Gao, Q. Lu, X. Liu, Y. Yan, D. Zhao, Nano Lett. 1 (2001) 743.
[140] B. Folch, J. Larionova, Y. Guari, C. Guérin, A. Mehdi, C. Reyé, J. Mater. Chem. 14 (2004) 2703.
[141] A. Fukuoka, T. Higuchi, T. Ohtake, T. Oshio, J. Kimura, Y. Sakamoto, N. Shimomura, S. Inagaki, M. Ichikawa, Chem. Mater. 18 (2006) 337.
[142] Y. Wu, T. Livneh, Y.X. Zhang, G. Cheng, J. Wang, J. Tang, M. Moskovits, G.D. Stucky, Nano Lett. 4 (2004) 2337.

[143] H. Song, R.M. Rioux, J.D. Hoefelmeyer, R. Komor, K. Niesz, M. Grass, P. Yang, G.A. Somorjai, J. Am. Chem. Soc. 128 (2006) 3027.
[144] N.K. Mal, M. Fujiwara, Y. Tanaka, Nature 421 (2003) 350.
[145] N.K. Mal, M. Fujiwara, Y. Tanaka, T. Taguchi, M. Matsukata, Chem. Mater. 15 (2003) 3385.
[146] C.-Y. Lai, B.G. Trewryn, D.M. Jeftinija, K. Jeftinija, S. Xu, S. Jeftinija, V.S.-Y. Lin, J. Am. Chem. Soc. 125 (2003) 4451.
[147] D.R. Radu, C.-Y. Lai, J.W. Wiench, M. Pruski, V.S.-Y. Lin, J. Am. Chem. Soc. 126 (2004) 1640.
[148] B.G. Trewyn, C.M. Whitman, V.S.-Y. Lin, Nano Lett. 4 (2004) 2139.
[149] D.R. Radu, C.-Y. Lai, K. Jeftinija, E.W. Rowe, S. Jeftinija, V.S.-Y. Lin, J. Am. Chem. Soc. 126 (2004) 13216.
[150] I. Slowing, B.G. Trewyn, V.S.-Y. Lin, J. Am. Chem. Soc. 128 (2006) 14792.
[151] R. Casasús, E. Aznar, M.D. Marcos, R. Martínez-Máñez, F. Sancenón, P. Amorós, Angew. Chem. Int. Ed. 45 (2006) 6661.
[152] R. Hernandez, H.-R. Tseng, J.W. Wong, J.F. Stoddart, J.I. Zink, J. Am. Chem. Soc. 126 (2004) 3370.
[153] T.D. Nguyen, H.-R. Tseng, P.C. Celestre, A.H. Flood, Y. Liu, J.F. Stoddart, J.I. Zink, Proc. Natl. Acad. Sci. 102 (2005) 10029.
[154] R. Casasús, M.D. Marcos, R. Martínez-Máñez, R.V. Ros-Lis, J. Soto, L.A. Villaescusa, P. Amorós, D. Beltrán, C. Guillem, J. Latorre, J. Am. Chem. Soc. 126 (2004) 8612.
[155] Q. Yang, S. Wang, P. Fan, L. Wang, Y. Di, K. Lin, F.-S. Xiao, Chem. Mater. 17 (2005) 5999.
[156] F. Balas, M. Manzano, P. Horcajada, M. Vallet-Regí, J. Am. Chem. Soc. 128 (2006) 8116.
[157] J.C. Doadrio, E.M.B. Sousa, I. Izquierdo-Barba, A.L. Doadrio, J. Perez-Pariente, M. Vallet-Regí, J. Mater. Chem. 16 (2006) 462.
[158] S. Giri, B.G. Trewyn, M.P. Stellmaker, V.S.-Y. Lin, Angew. Chem. Int. Ed. 44 (2005) 5038.
[159] J. Kim, J.E. Lee, J.H. Yu, B.C. Kim, K. An, Y. Hwang, C.-H. Shin, J.-G. Park, J. Kim, T. Hyeon, J. Am. Chem. Soc. 128 (2006) 688.
[160] H.-J. Kim, J.-E. Ahn, S. Haam, Y.-G. Shul, S.-Y. Song, T. Tatsumi, J. Mater. Chem. 16 (2006) 1617.
[161] T. Sen, A. Sebastianelli, I.J. Bruce, J. Am. Chem. Soc. 128 (2006) 7130.
[162] Y. Wang, F. Caruso, Chem. Mater. 17 (2005) 953.
[163] Y. Wang, F. Caruso, Chem. Mater. 18 (2006) 4089.
[164] Q. Zhang, K. Ariga, A. Okabe, T. Aida, Stud. Surf. Sci. Catal. 146 (2003) 465.
[165] Q. Zhang, K. Ariga, A. Okabe, T. Aida, J. Am. Chem. Soc. 126 (2004) 988.
[166] W. Otani, K. Kinbara, Q. Zhang, K. Ariga, T. Aida, Chem. Eur. J. 13 (2007) 1731.
[167] C. Tourné-Péteilh, D. Brunel, S. Bégu, B. Chiche, F. Fajula, D.A. Lerner, J.-M. Devoisselle, New. J. Chem. 27 (2003) 1415.
[168] L. Washmon-Kriel, V.L. Jimenez, K.J. Balkus Jr., J. Mol. Catal. B-Enzym. 10 (2000) 453.
[169] H. Takahashi, B. Li, T. Sasaki, C. Miyazaki, T. Kajino, S. Inagaki, Chem. Mater. 12 (2000) 3301.
[170] Y. Wei, J. Xu, Q. Feng, M. Lin, H. Dong, W.-J. Zhang, C. Wang, J. Nanosci. Nanotechnol. 1 (2001) 83.
[171] H.H.P. Yiu, C.H. Botting, N.P. Botting, P.A. Wright, Phys. Chem. Chem. Phys. 3 (2001) 2983.
[172] H.H.P. Yiu, P.A. Wright, N.P. Botting, Micropor. Mesopor. Mater. 44/45 (2001) 763.
[173] H. Takahashi, B. Li, T. Sasaki, C. Miyazaki, T. Kajino, S. Inagaki, Micropor. Mesopor. Mater. 44/45 (2001) 755.
[174] T. Sasaki, T. Kajino, B. Li, H. Sugiyama, H. Takahashi, Appl. Environ. Microbiol. 67 (2001) 2208.
[175] J. Deere, E. Magner, J.G. Wall, B.K. Hodnett, Chem. Commun. (2001) 465.
[176] J. Deere, E. Magner, J.G. Wall, B.K. Hodnett, J. Phys. Chem. B 106 (2002) 7340.
[177] Y.-J. Han, J.T. Watson, G.D. Stucky, A. Butler, J. Mol. Catal. B-Enzym. 17 (2002) 1.
[178] J. Deere, E. Magner, J.G. Wall, B.K. Hodnett, Catal. Lett. 85 (2003) 19.
[179] A.S.M. Chong, X.S. Zhao, Appl. Surf. Sci. 237 (2004) 398.
[180] D. Goradia, J. Cooney, B.K. Hodnett, E. Magner, J. Mol. Catal. B-Enzym. 32 (2005) 231.
[181] M. Hartmann, Chem. Mater. 17 (2005) 4577.
[182] J.F. Díaz, K.J. Balkus Jr., J. Mol. Catal. B-Enzym. 2 (2006) 115.
[183] Y. Han, S.S. Lee, J.Y. Ying, Chem. Mater. 18 (2006) 643.
[184] A. Vinu, V. Murugesan, M. Hartmann, J. Phys. Chem. B 108 (2004) 7323.
[185] A. Vinu, V. Murugesan, O. Tangermann, M. Hartmann, Chem. Mater. 16 (2004) 3056.
[186] A. Vinu, V. Murugesan, W. Böhlmann, M. Hartmann, J. Phys. Chem. B 108 (2004) 11496.
[187] M. Miyahara, A. Vinu, K.Z. Hossain, T. Nakanishi, K. Ariga, Thin Solid Films 499 (2006) 13.
[188] M. Miyahara, A. Vinu, K. Ariga, J. Nanosci. Nanotechnol. 6 (2006) 1765.
[189] M. Miyahara, A. Vinu, T. Nakanshi, K. Ariga, Kobunshi Ronbunshu 61 (2004) 623.
[190] A. Vinu, M. Miyahara, K. Ariga, J. Phys. Chem. B 109 (2005) 6436.
[191] A. Vinu, M. Myahara, K.Z. Hossain, T. Nakanishi, K. Ariga, Stud. Surf. Sci. Catal. 156 (2005) 637.
[192] M. Hartmann, A. Vinu, G. Chandrasekar, Chem. Mater. 17 (2005) 829.
[193] G. Chandrasekar, A. Vinu, V. Murugesan, M. Hartmann, Stud. Surf. Sci. Catal. 158 (2005) 1169.
[194] A. Vinu, K.Z. Hossain, G.S. Kumar, K. Ariga, Carbon 44 (2006) 530.
[195] A. Vinu, K.Z. Hossain, G.S. Kumar, V. Sivamurugan, K. Ariga, Stud. Surf. Sci. Catal. 156 (2005) 631.
[196] X. Hu, S. Spada, S. White, S. Hudson, E. Magner, J.G. Wall, J. Phys. Chem. 110 (2006) 18703.
[197] S.M. Solberg, C.C. Landry, J. Phys. Chem. 110 (2006) 15261.
[198] M. Luechinger, A. Kienhöfer, G.D. Pirngruber, Chem. Mater. 18 (2006) 1330.
[199] C.-H. Lee, S.-T. Wong, T.-S. Lin, C.-Y. Mou, J. Phys. Chem. B 109 (2005) 775.
[200] Y. Astutli, E. Topoglidis, P.B. Briscoe, A. Fantuzzi, G. Gilardi, J.R. Durrant, J. Am. Chem. Soc. 126 (2004) 8001.
[201] T. Itoh, K. Yano, Y. Inada, Y. Fukushima, J. Am. Chem. Soc. 124 (2002) 13437.
[202] T. Itoh, K. Yano, T. Kajino, S. Itoh, Y. Shibata, H. Mino, R. Miyamoto, Y. Inada, S. Iwai, Y. Fukushima, J. Phys. Chem. B 108 (2004) 13683.
[203] J.R. Stromberg, J.D. Wnuk, R.A.F. Pinlac, G.J. Meyer, Nano Lett. 6 (2006) 1284.
[204] S. Asaftei, L. Walder, Langmuir 22 (2006) 5544.
[205] M.M. Tomczak, D.D. Glawe, L.F. Drummy, C.G. Lawrence, M.O. Stone, C.C. Perry, D.J. Pochan, T.J. Deming, R.R. Naik, J. Am. Chem. Soc. 127 (2005) 12577.
[206] K. Ariga, T. Aimiya, Q. Zhang, A. Okabe, M. Niki, T. Aida, Int. J. Nanosci. 1 (2002) 521.
[207] K. Ariga, Q. Zhang, M. Niki, A. Okabe, T. Aida, Stud. Surf. Sci. Catal. 146 (2003) 427.
[208] K. Ariga, Chem. Rec. 3 (2004) 297.
[209] Y. Fujii, Y. Hasegawa, S. Yanagida, Y. Wada, Chem. Commun. (2006) 3065.
[210] M. Álvaro, N. Benitez, D. Das, B. Ferrer, H. García, Chem. Mater. 16 (2004) 2222.
[211] S.Y. Choi, M. Mamak, N. Coombs, N. Chopra, G.A. Ozin, Nano Lett. 4 (2004) 1231.
[212] S. Gago, J.A. Fernandes, J.P. Rainho, R.A.S. Ferreira, M. Pillinger, A.A. Valente, T.M. Santos, L.D. Carlos, P.J.A. Ribeiro-Claro, J.S. Conçalves, Chem. Mater. 17 (2005) 5077.
[213] X. Guo, L. Fu, H. Zhang, L.D. Carlos, C. Peng, J. Guo, J. Yu, R. Deng, L. Sun, New J. Chem. 29 (2005) 1351.
[214] A. Okabe, T. Fukushima, K. Ariga, T. Aida, Angew. Chem. Int. Ed. 41 (2002) 3414.
[215] T.-Q. Nguyen, J. Wu, V. Doan, B.J. Schwartz, S.H. Tolbert, Science 288 (2000) 652.
[216] M.J. MacLachlan, M. Ginzburg, N. Coombs, N.P. Raju, J.E. Greedan, G.A. Ozin, I. Manners, J. Am. Chem. Soc. 122 (2000) 3878.
[217] M.S. Cho, H.J. Choi, W.-S. Ahn, Langmuir 20 (2004) 202.
[218] J. Jang, B. Lim, J. Lee, T. Hyeon, Chem. Commun. (2001) 83.
[219] T. Aida, K. Tajima, Angew. Chem. Int. Ed. 40 (2001) 3803.

[220] M. Ikegame, K. Tajima, T. Aida, Angew. Chem. Int. Ed. 42 (2003) 2154.
[221] G. Li, S. Bhosale, T. Wang, Y. Zhang, H. Zhu, J.-H. Fuhrhop, Angew. Chem. Int. Ed. 42 (2003) 3818.
[222] Y. Lu, Y. Yang, A. Sellinger, M. Lu, J. Huang, H. Fan, R. Haddad, G. Lopez, A.R. Burns, D.Y. Sasaki, J. Shelnutt, C.J. Brinker, Nature 410 (2001) 913.
[223] V.S.-Y. Lin, D.R. Radu, M.-K. Han, W. Deng, S. Kuroki, B.H. Shanks, M. Pruski, J. Am. Chem. Soc. 124 (2002) 9040.
[224] A.P.-Z. Clark, K.-F. Shen, Y.F. Rubin, S.H. Tolbert, Nano Lett. 5 (2005) 1647.
[225] H. Peng, J. Tang, L. Yang, J. Pang, H.S. Ashbaugh, C.J. Brinker, Z. Yang, Y. Lu, J. Am. Chem. Soc. 128 (2006) 5304.
[226] M. Alvaro, M. Benitez, D. Das, H. Garcia, E. Peris, Chem. Mater. 17 (2005) 4958.
[227] K. Tajima, L.-S. Li, S.I. Stupp, J. Am. Chem. Soc. 128 (2006) 5488.
[228] J.R. Herance, E. Peris, J. Vidal, J.L. Bourdelande, J. Marquet, H. García, Chem. Mater. 17 (2005) 4097.
[229] W.C. Molenkamp, M. Watanabe, H. Miyata, S.H. Tolbert, J. Am. Chem. Soc. 126 (2004) 4476.
[230] A.G. Pattantyus-Abraham, M.O. Waif, Chem. Mater. 16 (2004) 2180.
[231] O.Yu. Posudievsky, G.M. Telbiz, V.K. Rossokhaty, J. Mater. Chem. 16 (2006) 2485.
[232] E.L. Clennan, Coord. Chem. Rev. 248 (2004) 477.
[233] T. Yui, T. Tsuchino, T. Itoh, M. Ogawa, Y. Fukushima, K. Takagi, Langmuir 21 (2005) 2644.
[234] D.F. Rohlfing, J. Rathouský, Y. Rohlfing, O. Bartels, M. Wark, Langmuir 21 (2005) 11320.
[235] E. Martinez-Ferrero, D. Grosso, C. Boissière, C. Sanchez, O. Oms, D. Leclercq, A. Vioux, F. Momandre, P. Audebert, J. Mater. Chem. 16 (2006) 3762.
[236] M. Zukalová, A. Zukal, L. Kavan, M.K. Nazeeruddin, P. Liska, M. Grätzel, Nano Lett. 5 (2005) 1789.
[237] J. Fan, T. Wang, C. Yu, B. Tu, Z. Jiang, D. Zhao, Adv. Mater. 16 (2004) 1432.
[238] G.S. Chai, I.S. Shin, J.-S. Yu, Adv. Mater. 16 (2004) 2057.